Comparative phylogeography of chloroplast and nuclear DNA markers reveals ancient and present hybridization in the Mediterranean *Helichrysum pendulum* complex (Compositae)

Sonia Herrando Moraira

Supervisors

Dr. Mercè Galbany Casals
Department of Animal Biology, Plant Biology and Ecology

Dr. Roser Vilatersana Lluch
Botanical Institute of Barcelona (IBB-CSIC-ICUB)

Master's Degree in Terrestrial Ecology and Biodiversity Management
Terrestrial Ecology specialisation
Universitat Autònoma de Barcelona

16 September 2014

Master's Degree in Terrestrial Ecology and Biodiversity Management

Terrestrial Ecology specialisation

Universitat Autònoma de Barcelona

Comparative phylogeography of chloroplast and nuclear DNA markers reveals ancient and present hybridization in the Mediterranean *Helichrysum pendulum* complex (Compositae)

Dr. Mercè Galbany Casals
Department of Animal Biology, Plant Biology and Ecology
Universitat Autònoma de Barcelona

Dr. Roser Vilatersana Lluch
Botanical Institute of Barcelona
(IBB-CSIC-ICUB)

Sonia Herrando Moraira

16 September 2014

Journal

Molecular Phylogenetics and Evolution

Work information

Star working: October 2013

	Student participation
Laboratory work	• Half conducted by the student (ETS marker) • During the months of October to March was attempted to obtain AFLP markers for use in this work. But ultimately they could not be included due to time limitation.
Data Analysis	• Completely by the student
Results interpretation	• Completely by the student (advised by the supervisors)
Manuscript writing	• Completely by the student (advised by the supervisors)

Comparative phylogeography of chloroplast and nuclear DNA markers reveals ancient and present hybridization in the Mediterranean *Helichrysum pendulum* complex (Compositae)

Sonia Herrando Moraira

Abstract

The geological and climatic history of the Mediterranean basin over the last 6 million years has been determinant in shaping current geographic distribution of genetic variation in organisms. Phylogeographical approaches are considered one of most useful analysis for unraveling the evolutionary history of species. The *Helichrysum pendulum* complex is a group of three closely related plant species distributed in several islands and isolated continental localities of the Western-Central Mediterranean basin, providing an ideal case of study to analyze the processes involved in modelling its current genetic structure. Two cpDNA region rpl32-trnL intergenic spacer and the nrDNA region ETS were sequenced for 1-8 individuals from each of the 44 total populations sampled, covering the whole geographic range of the complex. Our results suggest that the complex originated in northern Africa and colonized several islands and continental areas of the northern Basin through the Gibraltar and Sicilian straits during phases of low sea level, favored by long distance dispersal events. While ETS data suggest a model of isolation by distance and show a main genetic barrier between populations of Western and Central Mediterranean areas, the rpl32-trnL reveals the existence of two divergent and not geographically structured haplotype groups within the complex. Ancient hybridization events among lineages of sect. *Stoechadina* are suggested as the most plausible cause for the haplotypes pattern observed, while several evidences of current hybridization between *H. pendulum* and several species of sect. *Stoechadina* are also detected in ETS data.

Keywords

ETS, reticulate evolution, rpl32-trnL, straits, Western-Central Mediterranean basin

1. Introduction

Understanding present and historical processes that have influenced current plant distribution patterns and genetic structure of species is one of the most challenging goals of phylogeography (Avise, 2000). In the last 15 years, phylogeography has benefited tremendously from the application of DNA-methods (Lo Presti and Oberprieler, 2011), a newly developed technique with the ability to obtain DNA sequence variation from numerous individuals and to reconstruct phylogenies based on these sequences.

Gene flow among populations, genetic drift, founder effects and life-history traits are necessary but not enough to explain the distribution and diversity of species (Troia et al., 2012). Two other factors are decisive elements in the shaping of plant species distribution: geological history and climate variations (Thompson, 2005). Over the past 6 Ma, all parts of the Mediterranean basin underwent several dramatic changes (Woodward, 2009): the desiccation of the Mediterranean Sea in the Messinian Salinity Crisis (MSC) (5.96–5.33 Ma; Hsü et al., 1977), followed by the establishment of the Mediterranean climate during the Pliocene (~3 Ma) (Thompson, 2005) and oscillations in climate and sea level during glacial and interglacial periods in Quaternary period (Blondel and Aronson, 1999). All those events were determinant factors in floristic composition and genetic variation of Mediterranean taxa (Thompson, 2005). During the MSC, the strait of Gibraltar was closed (Hsü et al., 1977), and Mediterranean sea-level dropped in consequence of intense evaporation. Subsequently, a desert territory was emerged allowing the establishing of land bridges between southern Europe and northern Africa (Duggen et al., 2003) and between some of the islands of the Mediterranean basin (Beerli et al., 1996). This transition area promoted the migration and colonization of new territories by organisms that, otherwise, would have remained within narrower geographical areas because of intrinsic biological limitations. The subsequent refilling of the Mediterranean basin following the reopening of the Strait of Gibraltar brought about the irreversible geographical fragmentation of those organisms that used the Mediterranean basin to expand their range (Beerli et al., 1996).

Along the Mediterranean basin, the MSC has been widely classically invoked as the fundamental cause for land connections across several straits, which have been considered important modulators of phylogeography (Nieto-Feliner, 2014). It is known that straits in the Mediterranean basin have been used as a bridge or barrier to dispersal by many plant species. The Strait of Gibraltar is one of such areas. Currently formed by two facing peninsulas, it has intermittently separated the landmasses of Europe and Africa on the western Mediterranean extreme since their collision in the late Miocene (Duggen et al., 2003). However, the role of this strait as a biogeographic barrier or bridge differs among plant species. On the one hand, the 14 km of open sea of the Strait of Gibraltar have been shown to be sufficient to cause significant genetic differentiation among populations separated by it (Fiz et al., 2002; Terrab et al., 2008). On the other hand, gene flow between populations at both sides of this strait has also been documented in different phylogeographic studies (Ortiz et al., 2007; Guzmán and Vargas, 2009). The narrow and shallow Sicilian Channel has had the same role as the Strait of Gibraltar, and its impact in the distribution of genetic variation has been made evident in several studies (Lo Presti and Oberprieler, 2011; Troia et al., 2012). During the Pleistocene, sea-level oscillations facilitated biotic exchange between Sicily and Tunisia (Fernández-Mazuecos and Vargas, 2011; Lo Presti and Obeprieler, 2011). According to several researches, genetic exchanges between animal (Stöck et al., 2008) or plant populations (Troia et al., 2012) were ascribed to a land-bridge between the two regions, but also to long-distance dispersal events in other cases (Fernández-Mazuecos and Vargas, 2011; Hilpold et al., 2011).

Recently, a number of phylogeographical studies using molecular methods have focused on plants from several Mediterranean island systems, providing an understanding of the effects of geographical isolation and long-term fragmentation on population divergence and speciation (e.g. Molins et al., 2011). The western and central Mediterranean island systems provide one of the best natural laboratories. Whereas some islands have ancient continental origin (Balearic Islands, Sardinia and Corsica), others have very recent volcanic origin (Pantelleria). It is also interesting that, during the Pleistocene sea-level shifts, some of these islands have been connected between them or to the mainland allowing gene flow between populations, e.g. between Sicily and Tunisia and also between Sicily and other islands of the region, such as Malta, Pantelleria, Lampedusa, and the Aeolian and Aegadian archipelagos (Fernández-Mazuecos and Vargas, 2011; Lo Presti and Oberprieler, 2011). In contrast, other archipelagos have remained isolated since the opening of theGibraltar Strait (5.3 Ma), such as the Balearic Islands, providing different historical scenarios that may have shaped the present distribution of genetic variation.

The present work focuses on a group of closely related species belonging to the genus *Helichrysum* Mill. (Gnaphalieae, Compositae), the *Helichrysum pendulum* complex. According to a recent taxonomic study comprising the complex in its entire distribution area (Galbany-Casals et al., 2006), it comprises three sub-shrubby to shrubby perennial species: *Helichrysum pendulum* (C. Presl) C. Presl, *Helichrysum valentinum* Rouy and *Helichrysum errerae* Tineo. All of these taxa belong to sect. *Stoechadina* (DC.) Gren. & Godr. (Galbany-Casals et al., 2006), which constitutes a highly supported clade in nrDNA-based phylogenies (Galbany-Casals et al., 2009). *Helichrysum pendulum* has a west-central Mediterranean distribution and grows in the southern Iberian Peninsula (Gibraltar rock), the Balearic Islands (Majorca and Ibiza), Morocco, Algeria, Sardinia, Sicily and Malta (Galbany-Casals et al., 2006). *Helichrysum errerae* is endemic to Pantelleria Island (southwestern Sicily) and *H. valentinum* is endemic to the eastern Iberian Peninsula (Alicante province, Spain). With regards to ecological requirements, *H. pendulum* and *H. valentinum* usually grow on limestone rock cervices in mountain areas, in maritime cliffs, areas of scrubland and on karstic limestone plateaux above the cliffs (Galbany-Casals et al., 2006). In contrast, *H. errerae* grows in maritime volcanic rocks and cliffs (Galbany-Casals et al., 2006).

The *H. pendulum* complex is therefore an interesting group of study to analyze the relative contribution of geological, climatic and biological processes to its current distribution and genetic structure. It also provides a suitable model to study the impact of the Sicilian and Gibraltar straits as barriers or bridges to dispersion, and the role of mainland/island systems in the evolution of this Mediterranean species assemblage.

Hybridization is considered to have had an important role in the evolution of the genus *Helichrysum* (Galbany-Casals et al., 2012, 2014). Several studies have documented morphological intermediates or genetically similar populations between numerous pairs of sympatric species (Galbany-Casals et al., 2006, 2011, 2012). In fact, *H. valentinum* has been reported and interpreted as being of hybrid origin, as it exhibits an intermediate morphological appearance between *H. pendulum* and *H. stoechas* (L.) Moench. (Galbany-Casals et al., 2006). Up to date, however, contemporary and historical hybridization within the *H. pendulum* complex and with other taxa of the section has not been explored with molecular data.

For this research, two molecular markers have been used, the cpDNA rpl32-trnL intergenic spacer and the nrDNA External Transcribed Spacer (ETS) , which were chosen for two main reasons: (1) they often contain enough potential variation within and among plant species populations, consequently they are useful in analyses at low taxonomic levels (Baldwin and Markos, 1998); (2) they are available for many species of the genus *Helichrysum* because they have been used in previous phylogenetic analyses (Galbany-Casals et al., 2009, 2014).

The main objectives of this research are: (1) to unravel the genetic variation and phylogeographic patterns in the *H. pendulum* complex, and to ascertain which historical events in Mediterranean basin left detectable traces in the current genetic structure of this group of species; (2) to determine the impact of the Gibraltar and Sicilian straits in the differentiation or, alternatively, gene flow between populations; (3) to compare the phylogeographic patterns obtained with the two markers used given their different nature and mutation rate and (4) to test the effects of hybridization in present-day distribution of the genetic diversity found in this species complex.

2. Materials and methods

2.1. *Sampling strategy*

A total of 227 specimens from 44 populations belonging to the three species of the *Helichrysum pendulum* complex were collected, covering the entire distribution area of these species (see Figs. 1a, 2a and Table S1). One to eight individuals per population were sampled. To test the phylogenetic relationships and to identify possible hybridization events between the sampled populations of the *H. pendulum* complex and other species of the genus (see Table S1). The sampling was particularly focused on the rest of the species of sect. *Stoechadina* based on previous studies on morphology, phylogeny and hybridization (Galbany-Casals et al., 2009, 2012, 2014).

2.2. *DNA Extraction, amplification and sequencing*

Leaf material was collected in the field and immediately dried in silica gel. Total genomic DNA was extracted following the CTAB method of Doyle and Dickson (1987) with some modifications.

Amplification and sequencing of the ETS region was performed using the forward primer ETS1f (Linder et al., 2000) and the reverse primer 18S-ETS (Markos and Baldwin, 2001), and for the rpl32-trnL the forward primer rpl32F and the reverse primer trnL$^{(UAG)}$ (Shaw et al., 2007) were used. Polymerase chain reaction (PCR) amplifications were conducted following the reaction mixture described in Barres et al. (2011). The profiles used for amplification were as described in Galbany-Casals et al. (2009, 2010). Nucleotide sequencing was carried out at "Parque Científico de Madrid" on an ABI 3730 DNA analyzer (Applied Biosystems, Foster City, California, USA) or at the DNA Sequencing Core, CGRC/ICBR of the University of Florida on an ABI 3730xl DNA Analyzer (Applied Biosystems). In total, we included in the study 253 rpl32-trnL sequences, of which 229 are new, and 202 ETS sequences, of which 175 are new. Sequences obtained were edited using Chromas v.2.0 (Technelysium, Tewantin, Australia) and MEGA v.6 (Tamura et al., 2013) and each alignment was optimized with visual inspection and manual correction.

2.3 Data analyses

2.3.1. Network representation and phylogenetic analyses

For the rpl32-trnL a dataset was constructed with 216 specimens belonging to the *H. pendulum* complex. Several regions rich in poli-T and poli-A were manually excluded, as well as ambiguous positions. For the ETS, a dataset was constructed with 159 specimens belonging to the *H. pendulum* complex, in which ambiguous positions were also excluded. With both datasets a network of haplotypes and ribotypes was constructed using the statistical parsimony algorithm (Templeton et al., 1992) implemented in the software TCS v.1.21 (Clement et al., 2000), with 95% confidence limits. For these analyses, in the case of rpl32-trnL, indels were coded as discrete characters using the modified complex indel coding method implemented in SeqState v.1.4.1 (Müller, 2006), and in the case of the ETS, indels were considered as missing data given that sequences presented enough variation.

The phylogenetic relationships among the different haplotypes and ribotypes found in the TCS analyses were analysed separately using four additional species as outgroup taxa based on previous studies (Galbany-Casals et al., 2014). With these two datasets, dataset 1 (rpl32-trnL) and dataset 3 (ETS) (see Table 1), Bayesian inference (BI) and Maximum Parsimony (MP) phylogenetic analyses were performed separately. Bayesian inference analyses were performed with MrBayes v.3.1.2 (Ronquist and Huelsenbeck, 2003). The best-available model of molecular evolution was selected using the Akaike information criterion as implemented in the software jModel-Test v.0.0.1 (Posada, 2008). Two simultaneous and independent analyses of four Metropolis-coupled Markov chains were run for 5 million generations, starting from different random trees, and saving one out of every 500 generations. After checking the convergence of chains, the first 25% of the trees of each analysis were discarded (burn-in), which amply ensured the exclusion of trees that might have been sampled prior to the convergence of the Markov chains. A 50% majority-rule consensus tree was computed with MrBayes for the remaining trees. Posterior probability support (PP) was considered to be significant for nodes with PP ≥ 0.95. Maximum Parsimony Bootstrap analyses (Felsenstein, 1985) were performed with PAUP v.4.0b10 (Swofford, 2002) with 1000 replicates, random taxon addition with 10 replicates, and no branch-swapping. Parsimony uninformative characters were excluded in order to standardize parsimony statistics. Bootstrap support (BS) values were considered to be significant for nodes with BS ≥ 70%. To evaluate relative robustness of the clades found in the most parsimonious trees, consistency index (CI), retention index (RI) and rescaled consistency index (RC) were calculated with PAUP software.

2.3.2. Genetic diversity and geographical structure analyses

Genetic diversity parameters were computed using DnaSP v.5 software (Librado and Rozas, 2009): number of polymorphic (segregating) sites (S), number of unique haplotypes/ribotypes (H), haplotype/ribotype diversity (Hd) and nucleotic diversity (π) excluding gaps and ambiguous positions. The geographical structure of genetic variation was assessed by an analyses of molecular variance (AMOVA) following the approach of Excoffier et al. (1992) using the program ARLEQUIN v.3.5.1.2 (Excoffier and Lischer, 2009). The AMOVA analyses were performed at different hierarchical levels. The significance levels of the variance components were obtained by nonparametric permutation using 10,000 replicates. The

genetic differentiation parameters among populations (G_{ST}, N_{ST}) were estimated with the program PERMUT v.1.0 (Pons and Petit, 1996). The existence of phylogeographical structure was tested by comparing the differences between G_{ST} and N_{ST} values with a permutation test that used 10,000 permutations. Due to software limitations, only populations with more than three individuals were taken into account in this analysis. The existence of phylogeographical structure was also investigated with the Bayesian clustering method implemented in BAPS v.6.0 (Corander et al., 2008), choosing a spatial clustering algorithm and a mixture analysis of individuals with geographic information. We ran 10 replicates from each of the nine simulations from K = 2 to K = 10. The most likely K was chosen according to the highest log marginal likelihood [log (ml)] values. We examined the putative genetic barriers between populations using BARRIER v.2.2 (Manni et al., 2004). This software uses Monmonier's maximum-difference algorithm to compare geographic distances with Nei genetic distance between populations. The geographic distance matrix was generated by Geographic Distance Matrix Generator v.1.2.3 (Ersts, 2011) and the genetic distance matrix was obtained by GenAlEX v.6.5 (Peakall and Smouse, 2012).

2.3.3. Phylogenetic relationships with other species of the genus and the effects of hybridization

To test the phylogenetic relationships between the *H. pendulum* complex and other species of the genus and to identify possible hybridization events, the different haplotypes and ribotypes found in the *H. pendulum* complex from the TCS analyses were united to a broader sampling of rpl32-trnL (dataset 2) or ETS (dataset 4) sequences (see Table 1), respectively, which included a wide representation of species from sect. *Stoechadina*. In both cases, several unalignable regions were manually excluded. For the rpl32-trnL region indels were coded as discrete characters using the modified complex coding method implemented in SeqState v.1.4.1 (Müller, 2006), while for the ETS region indels were considered as missing data. With these two datasets BI and MP analyses were performed as described above, this time using *H. litorale* and *H. argyrosphaerum* as outgroup taxa based on Galbany-Casals et al. (2014). Finally, for the ETS, a Neighbour-Net (NN) analysis was also carried out using SplitsTree v.4.10 (Huson and Bryant 2006) with the default options including the ribotypes and the rest of species from sect. *Stoechadina*.

3. Results

3.1. Network representation and phylogenetic analyses

The alignments of the rpl32-trnL and the ETS datasets for the *Helichrysum pendulum* complex ranged from 855 to 870 bp (with a total aligned lenght of 927 bp) and from 880 to 884 bp (with a total aligned lenght of 884 bp), respectively.

A total of 15 haplotypes were identified in the *H. pendulum* complex (Fig. 1 and Table S1). Considering species separately, 14 of the haplotypes were found in *H. pendulum*, one of these (H1) shared with *H. errerae* and *H. valentinum*, whereas the haplotype H7 was only found in single population of *H. valentinum*. The most widely distributed haplotype was H1 (65.28% of all samples), whereas haplotypes H6-H8 were only found in one individual (Fig. 1a and Table S1). In most populations, a single haplotype was sampled. Only ten of the 44 populations presented several haplotypes, and seven of them contained one private haplotype. The network representing relationships among haplotypes inferred H1 to be the ancestral haplotype, and revealed a division between two main groups which did not correspond to a clear geographic division (Fig. 1b). One group comprised haplotypes H1-H8 and the other one haplotypes H10-H15, with haplotype H9 being in an intermediate position. These results were in accordance with the phylogenetic relationships among the haplotypes recovered in the BI and MP analyses (Table 1 and Fig. 1b), which also revealed a significant separation between the set of haplotypes H1 to H8 (BS = 98, PP = 1) and H10 to H15 (BS = 83, PP = 1), while the position of H9 was not resolved with statistical support.

A total of 44 ribotypes were identified in the *H. pendulum* complex (Table S1). Considering species separately, two exclusive ribotypes (R41-R42) were found in *H. errerae* and seven exclusive ribotypes (R1-R4 and R29-R31) were found in *H. valentinum* (Fig. 2 and Table S1). The rest of the ribotypes were found in *H. pendulum*, one of them (R7) also shared with *H. valentinum*. The most widely distributed ribotype was R39 (10.70% of all samples), whereas 20 ribotypes (12.58% of all samples) were only found in one individual (Table S1). In 20 populations, a single ribotype was sampled, whereas 22 populations were polymorphic. Twenty of the populations contained at least one private ribotype. To simplify the geographical representation of the ribotypes, they were classified in thirteen groups (Fig. 2a), based on the phylogenetic relationships among them obtained in the BI and MP analyses (Table 1 and Fig. 2b). The phylogenetic trees

showed a clear phylogeographical pattern (Table 1 and Fig. 2b). Three main supported clades were recovered: one clade comprising ribotypes R1-R20 (PP = 0.99, blue and green colours), distributed in the Western Mediterranean area; a second clade comprising ribotypes R33 to R44 restricted to the Sardinian and Sicilian locations (BS = 85, PP = 1, grey colour); and a third clade composed by ribotypes R21-R25 (PP = 1, brown and yellow colours), found in southern of Sicily, eastern Algeria and Malta. The position of the rest of the ribotypes and the relationships among these three main clades were not resolved.

3.2. Genetic diversity and geographical structure analyses

The genetic diversity values for each DNA marker are summarized in Table 2. The rpl32-trnL dataset contained 28 polymorphisms while the ETS dataset contained 35 polymorphisms. The ribotype diversity was higher than the haplotype diversity, which was moderate to low. Nucleotide diversity (π) presented similar low values for both markers. For the ETS region, N_{ST} was significantly higher than G_{ST} ($G_{ST} = N_{ST}$, $p < 0.05$), suggesting the existence of phylogeographical structure, whereas in the case of the rpl32-trnL spacer no phylogeographical structure was detected ($G_{ST} = N_{ST}$, $p > 0.05$). When no regional differentiation was considered, the AMOVA analyses showed that about 87.3% of the cpDNA variation in the *H. pendulum* complex was explained by differences among locations (Table 3). When regional differentiation in two groups (western and central Mediterranean) was assumed, genetic differentiation between them was very low (4.73%). Instead, a significant proportion of the variation was due to differences between more restricted geographical groups (68.52%). In the case of ETS, although most of the variation (88.19%) could be attributed to differences between populations as for the cpDNA marker, a great percentage of the variation was due to differences between the western and central groups (46.02%), and also between more restricted geographical groups (59.13%), supporting the existence of phylogeographical structure for this marker.

BAPS analyses identified $K = 2$ (log = -9745.149) for rpl32-trnL data and at $K = 3$ (log = -6307.362) for ETS data as the optimal number of genetically homogeneous groups. In the case of rpl32-trnL (Fig. 3a), most individuals from Morocco, Alicante, Balearic Islands, Algeria, Sicily, Marettimo and Pantelleria Islands were assigned to cluster 1; whereas all populations from Sardinia, Malta, Gibraltar and one population of Morocco (P10) were assigned to cluster 2. The only exception was population P2 from Majorca, with three individuals assigned to cluster 1 and two individuals assigned to cluster 2. In the BARRIER analysis (Fig. 3c) a first genetic barrier was inferred between Malta and the rest of populations. The ETS data showed a different pattern. In the BAPS analysis (Fig. 3b), cluster 1 contained the populations from western Mediterranean area, Malta, and some populations from Sicily; cluster 2 comprised most individuals from Sardinia, Sicily, Marettimo and Pantelleria Islands; and cluster 3 included several members scattered throughout both areas. In the BARRIER analysis (Fig. 3d), a first barrier for dispersion was inferred between the populations from the western and central Mediterranean areas, and a second barrier was inferred between the populations from Malta and Sicily that were included in cluster 1 in BAPS analysis, and the rest of populations of the central Mediterranean group.

3.3. Phylogenetic relationships with other species of the genus and the effects of hybridization

In the rpl32-trnL analyses (Fig. 4) neither the *H. pendulum* complex nor sect. *Stoechadina* were monophyletic. Haplotypes H1-H8 constituted a supported clade (BS = 95, PP = 1) together with representatives of *H. litoreum*, *H. crassifolium* and *H. stoechas* (mainly Iberian and Balearic populations). Haplotype 9 was closely related to *H. rubicundum* (PP = 0.98). Haplotypes H10 to H15 were grouped together without statistical support with all representatives of *H. italicum*. In the ETS analyses, the *H. pendulum* complex was not monophyletic, although all ribotypes were included in a main clade comprised by all species of sect. *Stoechadina* (BS = 94, PP = 1, Fig. 5). Within this section, none of the other species represented by several individuals was monophyletic neither. Both in the phylogenetic tree (Fig. 5) and the NN analysis (Fig. 6) ribotypes R33 to R44 were closely related to *H. litoreum*, *H. italicum* subsp. *italicum* and *H. italicum* subsp. *microphyllum*, while the rest of ribotypes (R1 to R32) were more related to *H. stoechas*. A geographic pattern was noted in the set of ribotypes related to *H. stoechas*. Ribotypes from western locations were closely related to the specimens of *H. stoechas* sampled in geographically close localities, whereas ribotypes from southern Sicily, eastern Algeria and Malta were grouped with specimens of *H. stoechas* from the eastern Mediterranean area (Crete and Rhodes).

4. Discussion

4.1. General phylogeographical patterns and processes in the Helichrysum pendulum *complex*

In a dated phylogeny of the tribe Gnaphalieae, Bergh and Linder (2009) suggested that the genus *Helichrysum* originated around 7 Ma ago. Even though this research only included South African species, the Mediterranean group has been inferred to be derived from African ancestors (Galbany-Casals et al., 2009, 2014). The resolution obtained in both the nrDNA and the cpDNA phylogenetic trees with regards to the *H. pendulum* complex is insufficient to infer the geographic origin of the group with confidence (Fig. 1b, Fig. 2b). However, given that our data show high values of haplotype and ribotype diversity in northern Africa together with a high number of private ribotypes and haplotypes, relative to the number of populations sampled, we hypothesize a northern Africa origin for the *H. pendulum* complex, which would agree with the geographical origin of the whole sect. *Stoechadina* (Galbany-Casals et al., 2009). The ancestor would have colonized the northern western and central Mediterranean regions during times of reduced distances between islands and continental land masses, either during the MSC or during the Pleistocene glaciations. However, long-distance dispersal events, favored by the excellent dispersal ability of the tiny achenes (~1 mm), cannot be ruled out as a possible interpretation for the complex expansion to areas isolated by the sea, e.g. the Balearic Islands, which have remained isolated since the opening of the Strait of Gibraltar (5.3 Ma; Thompson, 2005).

In this study, several incongruences were detected between the cpDNA and the nrDNA markers. In the case of the rpl32-trnL, two divergent haplotype groups that differ from each other by 12 mutational steps have been recovered (Fig. 1), also identified by BAPS analysis (Fig. 3a). When analysed together with other species of the genus, haplotypes H1 to H8 appear to be closely related to *H. stoechas,* whereas haplotypes H10 to H15 are related to *H. italicum* (Fig. 4). Ancestral hybridization and subsequent introgression seem to be the most likely hypothesis to explain the pattern observed in Sardinia, where all individuals present haplotypes H12-H14, and *H. pendulum* and *H. italicum* coexist. Ancient chloroplast capture would had occurred and consequently chloroplast genome of *H. pendulum* would have extinguished in this region. To favor that plausible hypothesis the following potential reasons were found: (1) reticulation and chloroplast capture occur in taxa with recent speciation and at low taxonomic levels (Sang and Zhong, 2000); (2) past interspecific hybridization within the genus *Helichrysum* has been suggested by molecular data (Galbany-Casals et al., 2009, 2014), showing biologically possible reticulation events; (3) similar cases of chloroplast capture between rather divergent taxonomic groups are also known from other plants (Jackson et al., 1999; Fehrer et al., 2007). The rest of haplotypes from group H10-H15 were detected in Morocco, Gibraltar, Majorca and Malta. Hybridization would be also the most plausible explanation, although the limited sampling prevents us to distinguish between ancient or present hybridization.

Opposite to the absence of phylogeographical structure (Table 3) and the lack of geographic pattern found in the cpDNA marker (Fig. 1a) the general distribution of ribotypes present genetic similarities between geographically close localities (Fig. 2a), suggesting a possible model of isolation by distance (Nieto-Feliner, 2014). Gene flow between nearest populations would have been facilitated by land bridges or reduced distances among several land masses during Pleistocene glacial phases (Thompson, 2005). A similar model was also detected in a phylogeographic study of the Mediterranean *Helichrysum italicum* Galbany-Casals et al. (2010), for which the importance of gene flow and genetic affinities between nearest populations was highlighted. Additionally, analyses of ETS data revealed relative genetic isolation between western and central Mediterranean areas. The moderately high percentage of the variation was found between western and central groups (46.02%; Table 3), which share a low number of ribotypes (Fig. 2 and Table S1), and are separated by the first genetic barrier detected by Barrier analysis (Fig. 3d).

One of the main coincidences between rpl32-trnL and ETS data is that genetic variation was mostly attributed to differences between populations (87.30% for rpl32-trnL, 88.19% for ETS). High genetic differentiation among populations is probably consequence of the habitat of these species. The probability to receive seed dispersal from a neighboring cliff population is low. Habitat barriers produced in cliffs contribute to a progressive reproductive isolation between populations. The second coincidence between both markers is the strong genetic differentiation of Maltese populations respect to all other populations. These populations were characterized by the presence of an exclusive haplotype (H15), which was separated by seven mutational steps from the nearest one (Fig. 1a). Additionally the first genetic barrier for dispersion was detected between Malta and the rest of populations (Fig. 3c). These results agree with the detection of unique haplotypes in Maltese populations of *Athemis secundirramea* (Lo Presti and Oberprieler, 2011). Our results could suggest an ancient colonization of Malta, followed by genetic drift due to long isolation of the

island from other regions. Additionally, the pattern of ribotypes testifies about the existence of genetic affinities between the populations from southern Sicily and Malta. These affinities between the Maltese and the Sicilian flora and fauna have been well documented by other researchers (Junikka et al., 2006) and have been attributed to gene flow during Quaternary glaciations when sea-level decreased. These connections were interrupted between 4 and 2 Ma during warm periods of the Pleistocene, and in the Holocene (Pfenninger et al., 2010). The current isolation of Malta populations from the remainder *H. pendulum* complex could be illustrated by the unique set of ribotypes (R24-R25) detected in Malta populations (Fig. 2a). The Maltese populations have been considered an independent taxon by several authors (Pignatti, 1979; Brullo et al., 1988), and genetic results would support this view, although detailed studies of the whole complex based on morphology would be needed to establish the most suitable taxonomic status.

In contrast to the high genetic differentiation of the Maltese populations, we found low levels of genetic diversity in *H. errerae* populations from Pantelleria, which are very closely related to *H. pendulum*. This is in accordance with the recent emergence of Pantelleria Island dated from 114 ka (Wallmann et al., 1988). Since its formation, Pantelleria has never been connected to Sicily or Tunisia. Only during the Last Glacial Maximum (19–22 ka; Yokoyama et al., 2000) Pantelleria was separated from Sicily only by a shallow strait, which could have favored gene flow between Sicily and Pantelleria populations. The two exclusive ribotypes detected in Pantelleria (R41-R42) indicate the current genetic isolation of these populations, in agreement with a notable morphological differentiation from *H. pendulum* and a local adaptation to volcanic rocks instead of limestone substrates (M. Galbany-Casals, pers. obser.). The genetic affinities of *H. errerae* with one ribotype detected in southern Sicily (R40) (Fig. 2b), suggest a Sicilian origin for *H. errerae*. Furthermore, Pantelleria ribotypes are closely related to R43 found in the population of *H. pendulum* sampled in Marettimo Island. Similar results were obtained in a previous work performed with AFLP for *H. pendulum* in Sicily (Scialabba et al., 2008), which lead those authors to consider populations from Marettimo and from Pantelleria islands the same species, with two varieties (*H. errerae* var. *messeri* for Marettimo and *H. errerae* var. *errerae* for Pantelleria).

4.2. The impact of the Gibraltar and Sicilian straits on the genetic structure of Helichrysum pendulum *complex*

The geographic proximity of land masses at both sides of the Strait of Gibraltar appears to have played a significant role in the genetic exchange between populations in the *H. pendulum* complex. In particular, our results show an exclusive haplotype (H10) shared between populations at both sides of the strait (Fig. 1a), suggesting gene flow, as occurred in other plant groups (Ortiz et al., 2007; Arroyo et al., 2008). These results may indicate an ancient expansion of the *H. pendulum* complex across the Strait of Gibraltar, from North Africa to the Iberian Peninsula, while conditions remained favorable during periods of low sea level. In contrast, no ribotypes are shared between Gibraltar and Rif (Moroccan) populations, and the Gibraltar population bears an exclusive haplotype. These results support the hypothesis that the Strait of Gibraltar seems to have hindered the dispersion to some extent, resulting in recent genetic differentiation of the two facing populations. This is in agreement with other studies conducted across the Strait of Gibraltar in plant species (Terrab et al., 2007; Rubio de Casas et al., 2006).

With regards to the role of the Sicilian Strait, TCS and NN analysis of the ETS marker point out a genetic affinity between populations from southern Sicily and eastern Algeria (Figs. 1a, 2a and 4). The genetic affinity between populations from these locations may be related to the presence of a land-bridge connection between Sicily and Northeast Africa at different times (Rosenbaum et al., 2002). Our data, which point to a relative higher genetic diversity in North African populations (compared to the Sicilian ones) in terms of number of haplotypes and ribotypes, might indicate a direction of the gene flow from Algeria towards Sicily, as suggested in other plant groups (e.g. Hipold et al., 2011; Lo Presti and Oberprieler, 2011). According to this assumption, the dispersal from northern Africa to Sicily likely occurred during cold periods of the Pleistocene when the distance between Tunisia and Sicily was much smaller, using land corridors or by means of stepping-stone islands, which could have been emerged during the glacial periods when the sea levels fell (Stöck et al., 2008), or via occasional long-distance dispersal (Cowie and Holland, 2006; Fernández-Mazuecos and Vargas, 2011).

4.3. Recent hybridization between the Helichrysum pendulum *complex and other taxa of the genus*

Present interspecific hybridization within the genus *Helichrysum* has been suggested in several works (Galbany-Casals et al., 2006, 2009, 2012). The role for hybridization in the case of the *H. pendulum* complex has been previously suggested by the frequent observation of morphological intermediates with other species of sect. *Stoechadina* (Galbany-Casals et al., 2006). Our results based on the ETS region show a general pattern in which geographically close interespecific populations appear as genetically related (Fig. 6), thus hybrids are locally produced between specimens belonging to different species that grow in the vicinity. This geographic pattern was noted in the sets of ribotypes related to *H. italicum* and *H. stoechas*. Firstly, in the western Mediterranean region, significant relationships between ribotypes of *H. valentinum* from Alicante (R1-R4) and *H. stoechas* from Lleida, relatively near to Alicante, were detected in the phylogenetic tree of the ETS region (Figs. 5 and 6). Furthermore, a connection between the rest of ribotypes detected in *H. valentinum* (R30-R32) and four specimens of *H. stoechas* sampled in Alicante and Ibiza was found, even though without statistical support (Figs. 5 and 6). Based on this molecular evidence, the possibility that *H. valentinum* might be a species of hybrid origin between *H. pendulum* and *H. stoechas*, as discussed in previous works (Galbany-Casals et al., 2006), is quite reasonable. Secondly, in the central Mediterranean region, hybridization events between *H. pendulum* and *H. stoechas* are suggested by the genetic similarities of the populations from eastern Algeria (R32) and southern Sicily (R21-R22) with four members of *H. stoechas* from Crete and Rhodes that were grouped in the same clade (Figs. 5 and 6). These results agree with previous observations of specimens with intermediate morphological appearance between *H. pendulum* and *H. stoechas* species both in Algeria and southern Sicily (Galbany-Casals et al., 2006). Some recent hybridization is also recognized between *H. pendulum* and *H. italicum* in areas were both species are sympatric, such as Sardinia and Sicily, suggested by the grouping of ribotypes (Figs. 5 and 6). These interpretation is supported by the previous observation of individuals with intermediate morphological features between these two species where they coexist (Galbany-Casals et al., 2006).

4.3. Conclusions

The two markers selected present different phylogeographical patterns, which compared provide a complete overview of the evolutionary history of the *H. pendulum* complex. In conclusion, our study provides evidences that this complex was originated in northern Africa and colonized the northern Mediterranean through the Gibraltar and Sicilian straits, effective geographical land bridges to gene flow during the MSC and Pleistocene glaciations. The nearest populations are those that exhibit more genetic similarities, although the Western and Central Mediterranean areas act as genetic barrier hampering the gene flow between these regions. Maltese populations have probably been genetically isolated for a long time from the rest of populations and their taxonomic status should be revised. Phylogeographic patterns of *H. pendulum* complex are strongly modulated by reticulate evolution with other species of sect. *Stoechadina*, produced by ancient and present hybridization events.

Acknowledgments

We are grateful to people who provided plant material from field collections. Financial support from the Spanish Ministerio de Ciencia e Inovación (CGL2010-18631/BOS) and the Catalan government (‘*Ajuts a grups consolidats’* 2009/SGR/00439) is also acknowledged.

References

Arroyo, J., Aparicio, A., Albaladejo, R.G., Muñoz, J., Braza, R., 2008. Genetic structure and population differentiation of the Mediterranean pioneer spiny broom *Calicotome villosa* across the Strait of Gibraltar. Biol. J. Linn. Soc. 93, 39–51.

Avise, J.C., 2000. Phylogeography. Harvard University Press, Boston.

Baldwin, B.G., Markos, S., 1998. Phylogenetic utility of the external transcribed spacer (ETS) of 18S–26S rDNA: congruence of ETS and ITS trees of *Calycadenia* (Compositae). Mol. Phylogenet. Evol. 10, 449–463.

Barres, L., Vilatersana, R., Molero, J., Susanna, A., Galbany-Casals, M., 2011. Molecular phylogeny of *Euphorbia* subg. *Esula* sect. *Aphyllis* (Euphorbiaceae) inferred from nrDNA and cpDNA markers with biogeographic insights. Taxon 60, 705–720.

Beerli, P., Hotz, H., Uzzell, T., 1996. Geologically dated sea barriers calibrate a protein clock for Aegean water frogs. Evolution 50, 1676–1687.

Bergh, N.G., Linder, H.P., 2009. Cape diversification and repeated out of southern-Africa dispersal in paper daisies (Asteraceae, Gnaphalieae). Mol. Phylogenet. Evol. 51, 5–18.

Blondel, J., Aronson, J., 1999. Biology and wildlife of the Mediterranean region. Oxford University Press, Oxford.

Brullo, S., Lanfranco, E., Pavone, P., Ronsisvalle, G., 1988. Taxonomical notes on the endemic flora of Malta. Giorn. Bot. Ital. 122, 9.

Clement M., Posada D., Crandall K.A., 2000. TCS: a computer program to estimate gene genealogies. Mol. Ecol. 9, 1657–1659.

Corander, J., Sirén, J., Arjas, E., 2008. Bayesian spatial modelling of genetic population structure. Comput. Stat. 23, 111–129.

Cowie, R.H., Holland, B.S., 2006. Dispersal is fundamental to biogeography and the evolution of biodiversity on oceanic islands. J. Biogeogr. 33, 193–198.

Doyle, J.J., Dickson, E.E., 1987. Preservation of plant samples for DNA restriction endonuclease analysis. Taxon 36, 715–722.

Duggen, S., Hoernle, K., van den Bogaard, P., Rüpke, L., Morgan, J.P., 2003. Deep roots of the Messinian salinity crisis. Nature 402, 602–606.

Ersts, P.J., 2011. Geographic Distance Matrix Generator (version 1.2.3). <http://biodiversityinformatics amnh org/open_source/gdmg>. (Accessed on 2014-8).

Excoffier, L., Smouse, P.E., Quattro J.M., 1992. Analysis of molecular variance inferred from metric distances among DNA haplotypes: Application to human mitochondrial DNA restriction data. Genetics 131, 479–491.

Excoffier, L., Lischer, H., 2009. Arlequin version 3.5.1.2 <http://cmpg.unibe.ch/software/arlequin3>. (Accessed on 2014-8).

Fehrer, J., Gemeinholzer, B., Chrtek, J., Bräutigam, S., 2007. Incongruent plastid and nuclear DNA phylogenies revel ancient intergeneric hybridization in *Pilosella* hawkweeds (*Hieracium*, Chichorieae, Asteraceae). Mol. Phylogenet. Evol. 42, 374–361.

Felsenstein, J., 1985. Confidence limits on phylogenies: An approach using the bootstrap. Evolution 39, 783–791.

Fernández-Mazuecos, M., Vargas, P., 2011. Historical isolation versus recent long-distance connections between Europe and Africa in bifid toadflaxes (*Linaria* sect. *Versicolores*). PLoS ONE 6, e22234.

Fiz, O., Valcárcel, V., Vargas, P., 2002. Phylogenetic position of Mediterranean Asteraceae and character evolution of daisies (*Bellis*, Asteraceae) inferred from nrDNA ITS sequences. Mol. Phylogenet. Evol. 25, 157–171.

Galbany-Casals, M., Andrés-Sánchez, S., Garcia-Jacas, N., Susanna, A., Rico, E., Martínez-Ortega, M.M., 2010. How many of Cassini anagrams should there be? Molecular systematics and phylogenetic relationships in the *Filago* group (Asteraceae, Gnaphalieae), with special focus on the genus *Filago*. Taxon 59, 1671–1689.

Galbany-Casals, M., Blanco-Moreno, J.M., Garcia-Jacas, N., Breitwieser, I., Smissen, R.D., 2011. Genetic and morphological variation in the Mediterranean *Helichrysum italicum* subsp. *microphyllum* (Asteraceae; Gnaphalieae). Plant Biol. 13, 678–687.

Galbany-Casals, M., Carnicero-Campany, P., Blanco-Moreno, J.M., Smissen, R.D., 2012. Morphological and genetic evidence of contemporary intersectional hybridization in *Helichrysum* (Asteraceae, Gnaphalieae). Plant Biol. 14, 789–800.

Galbany-Casals, M., Garcia-Jacas, N., Sáez, L., Benedí, C., Susanna, A., 2009. Phylogeny, biogeography, and character evolution in Mediterranean, Asiatic and Macaronesian *Helichrysum* (Asteraceae, Gnaphalieae) inferred from nuclear phylogenetic analyses. Int. J. Plant Sci. 170, 365–380.

Galbany-Casals, M., Sáez, L., Benedí, C., 2006. A taxonomic revision of *Helichrysum* Mill. sect. *Stoechadina* (DC.) Gren. & Godr. (Asteraceae, Gnaphalieae). Can. J. Bot. 84, 1203–1232.

Galbany-Casals, M., Unwin, M., Garcia-Jacas, N., Smissen R.D., Susanna, A., Bayer R.J., 2014. Phylogenetic relationships in *Helichrysum* (Compositae: Gnaphalieae) and related genera: Incongruence implications for generic delimitation. Taxon 63, 608–624.

Guzmán, B., Vargas P., 2009. Long distance colonisation by the Mediterranean *Cistus ladanifer* (Cistaceae) despite the absence of special dispersal mechanisms. J. Biogeogr. 36, 954–968.

Hilpold, A., Schönswetter, P., Susanna, A., Garcia-Jacas, N., Vilatersana, R., 2011. Evolution of the central Mediterranean *Centaurea cineraria* group (Asteraceae): evidence for relatively recent, allopatric diversification following transoceanic seed dispersal. Taxon 60, 528–538.

Hsü, K.J., Montardet, P., Bernoulli, D., Cita, M.B., Erickson, A., Garrison, R.E., Kidd, R., Mèlierés, F., Müller, C., Wright, R., 1977. History of the Mediterranean salinity crisis. Nature 267, 399–403.

Huson D.H., Bryant D., 2006. Application of phylogenetic networks in evolutionary studies. Mol. Biol. Evol. 23, 254–267.

Jackson, H.D., Steane, D.A., Potts, B.M., Vaillancourt, R.E., 1999. Chloroplast DNA evidence for reticulate evolution in *Eucalyptus* (Myrtaceae). Mol. Ecol. 8, 739–751.

Junikka, L., Uotila, P., Lahti, T., 2006. A phytogeographical comparison of the major Mediterranean islands on the basis of Atlas Florae Europaeae. Willdenowia 36, 379–388.

Librado, P., Rozas, J., 2009. DnaSP v5: software for comprehensive analysis of DNA polymorphism data. Bioinformatics 25, 1451–1452.

Linder, C.R., Goertzen, L.R., Heuvel, B.V., Francisco-Ortega, J., Jansen, R.K., 2000. The complete external transcribed spacer of 18S-26S rDNA: Amplification and phylogenetic utility at low taxonomic levels in Asteraceae and closely allied families. Mol. Phylogenet. Evol. 14, 285–303.

Lo Presti, R.M., Oberprieler, C., 2011. The central Mediterranean as a phytodiversity hotchpotch: phylogeographical patterns of the *Anthemis secundiramea* group (Compositae, Anthemideae) across the Sicilian Channel. J. Biogeogr. 38, 1109–1124.

Manni, F., Guerard, E., Heyer, E., 2004. Geographic patterns (genetic, morphologic, linguistic) variation: how barriers can be detected by using Monmonier's algorithm. Hum. Biol. 76, 173–190

Markos, S., Baldwin, B.G., 2001. Higher-level relationships and major lineages of *Lessingia* (Compositae, Astereae) based on nuclear rDNA internal and external transcribed spacers (ITS and ETS) sequences. Syst. Bot. 26, 168–183.

Molins, A., Bacchetta, G., Rosato, M., Roselló, J.A., Mayol, M., 2011. Molecular phylogeography of *Thymus herba-barona* (Laminaceae): Insight into evolutionary history of the flora of the western Mediterranean islands. Taxon 60, 1295–1305.

Müller, K., 2006. Incorporating information from length-mutational events into phylogenetic analysis. Mol. Phylogenet. Evol. 38, 667–676.

Nieto-Feliner, G., 2014. Patterns and processes in plant phylogeography in the Mediterranean Basin. A review. Perspect. Plant Ecol. Evol. Syst. (in press).

Ortiz, M.Á., Tremetsberger, K., Talavera, S., Stuessy, T., García-Castro, L., 2007. Population structure of *Hypochaeris salzmanniana* DC. (Asteraceae), an endemic species to the Atlantic coast on both sides of the Strait of Gibraltar, in relation to Quaternary sea level changes. Mol. Ecol. 16, 541–552.

Peakall, R., Smouse, P.E., 2012. GenAlEx 6.5: genetic analysis in Excel. Population genetic software for teaching and research-an update. Bioinformatics 28, 2537–2539.

Pfenninger, M., Véla, E., Jesse, R., Elejalde, M.A., Liberto, F., Magnin, F., Martínez-Ortí, A., 2010. Temporal speciation pattern in the western Mediterranean genus *Tudorella* P. Fischer, 1885 (Gastropoda, Pomatiidae) supports the Tyrrhenian vicariance hypothesis. Mol. Phylogenet. Evol. 54, 427–436.

Pignatti, S., 1979. Note critiche sulla Flora d'Italia. VI. Ultimi appunti miscellanei. Giorn. Bot. Ital. 113, 359-368.

Pons, O., Petit, R.J., 1996. Measuring and testing genetic differentiation with ordered versus unordered alleles. Genetics 144, 1237–1245.

Posada, D., 2008. jModelTest: Phylogenetic model averaging. Mol. Biol. Evol. 25, 1253–1256.

Ronquist, F., Huelsenbeck, J.P., 2003. MRBAYES 3: Bayesian phylogenetic inference under mixed models. Bioinformatics 19, 1572–1574.

Rosenbaum, G., Lister, G.S., Duboz, C., 2002. Reconstruction of the tectonic evolution of the western Mediterranean since the Oligocene. J. Virtual Explor. 8, 107–130.

Rubio de Casas, R., Besnard, G., Schönswetter, P., Balaguer, L., Vargas, P., 2006. Extensive gene flow blurs phylogeographic but not phylogenetic signal in *Olea europaea* L. Theor. Appl. Genet. 113, 575–583.

Sang, T., Zhong, Y., 2000. Testing hybridization hypotheses based on incongruent gene trees. Syst. Biol. 49, 422–434.

Scialabba, A., Agrimonti, C., Abbate, G.M., Marmiroli, N., 2008. Assessment of genetic variation in Sicilian *Helichrysum* (Asteraceae) and implications to germplasm conservation. Plant Biosys. 142, 287–297.
Shaw, J., Lickey, E.B., Schilling, E.E., Small, R.L., 2007. Comparison of whole chloroplast genome sequences to choose noncoding regions for phylogenetic studies in angiosperms: The tortoise and the hare III. Am. J. Bot. 94, 275–288.
Stöck, M., Sicilia, A., Belfiore, N.M., Buckley, D., Lo Brutto, S., Lo Valvo, M., Arculeo, M., 2008. Post Messinian evolutionary relationships across the Sicilian channel: mitochondrial and nuclear markers link a new green toad from Sicily to African relatives. BMC Evol. Biol. 8, 56.
Swofford, D.L., 2002. PAUP*: Phylogenetic analysis using parsimony (*and other methods), version 4.0 Beta. Sinauer, Sunderland
Tamura K., Stecher G., Peterson D., Filipski A., Kumar S., 2013. MEGA6: Molecular Evolutionary Genetics Analysis version 6.0. Mol. Biol. Evol. 30, 2725–2729.
Templeton, A.R., Crandall, K.A., Sing, C.F., 1992. A cladistic analysis of phenotypic associations with haplotypes inferred from restriction endonuclease mapping and DNA sequence data. III. Cladogram estimation. Genetics 123, 585–595.
Terrab, A., Schönswetter, P., Talavera, S., Vela, E., Stuessy, T.F., 2008. Range-wide phylogeography of *Juniperus thurifera* L., a presumptive keystone species of western Mediterranean vegetation during cold stages of the Pleistocene. Mol. Phylogenet. Evol. 48, 94–102.
Terrab, A., Talavera, S., Arista, M., Paun, O., Stuessy, T.F., Tremetsberger, K., 2007. Genetic diversity and geographic structure at chloroplast microsatellites (cpSSRs) in endangered West Mediterranean firs (*Abies* spp., Pinaceae). Taxon 56, 409–416.
Thompson, J.D., 2005. Plant evolution in the Mediterranean. Oxford University Press, Oxford.
Troia, A., Raimondo, F.M., Geraci, A., 2012. Does genetic population structure of *Ambrosina bassii* L. (Araceae, Ambrosineae) attest a post-Messinian land-bridge between Sicily and Africa?. Flora 207, 646–653.
Wallmann, P.C., Mahood, G.A., Pollard, D.D., 1988. Mechanical models for correlation of ring-fracture eruptions at Pantelleria, Strait of Sicily, with glacial sea-level drawdown. Bull. Volc. 50, 327–339.
Woodward, J.C., 2009. The physical geography of the Mediterranean. Oxford University Press, Oxford.
Yokoyama, Y., Lambeck, K., De Deckker, P., Johnston, P., Fifield, L.K., 2000. Timing of the Last Glacial Maximum from observed sea-level minima. Nature 406, 713–716.

Tables

Table 1
Characteristics of sequences and results of phylogenetic analyses for the rpl32-trnL intergenic spacer and ETS region

		rpl32-trnL spacer		ETS	
	Parameter	**Dataset 1**	**Dataset 2**	**Dataset 3**	**Dataset 4**
Characteristics of sequences	Number of sequences	19	53	48	85
	Length of sequences (bp)	790-835	769-835	839-1116	775-829
	Number of coded indels	14	21	—	—
	Total number characters	872	919	1119	849
	Informative characters % of total aligned length	24 2.71	44 4.68	87 7.77	184 21.67
Maximum parsimony	Number of maximum parsimony trees (MPTs)	14575	6876128	227477	125000
	Number of steps	28	80	131	505
	Consistency index (CI)	0.857	0.725	0.725	0.491
	Homoplasy index (HI)	0.143	0.275	0.275	0.509
	Retention index (RI) Rescaled consistency index (RC)	0.950 0.814	0.904 0.655	0.888 0.644	0.746 0.366
Bayesian inference	Sequence evolution model (AIC criteria)	GTR+G F81 (indels)	GTR+G+I F81 (indels)	GTR+G	GTR+G

Dataset 1 and dataset 3 correspond to haplotypes or ribotypes of the *Helichrysum pendulum* complex with outgroups. Dataset 2 and dataset 4 correspond to the *Helichrysum pendulum* complex analysed together with other species of the

Table 2
Genetic diversity and genetic differentiation parameters for the *Helichrysum pendulum* complex. Standard deviation is shown in some parameters

Parameter [1]	**rpl32-trnL spacer**	**ETS**
N	216	159
S	28	35
H	14	30
Hd	0.543 ± 0.0400	0.899 ± 0.0140
π	0.005 ± 0.0004	0.006 ± 0.0002
G_{ST}	0.798 ± 0.0624	0.572 ± 0.0698
N_{ST}	0.836 ± 0.0822	0.695 ± 0.0694

[1] N = sample size; S = number of polymorphic sites; H = number of haplotypes; Hd = haplotype diversity; π = nucleotide diversity

Table 3
Analyses of molecular variance (AMOVA) based on the rpl32-trnL spacer and ETS sequence data for the *Helichrysum pendulum* complex

		rpl32-trnL spacer				ETS			
	Sources of variation	df	Sum of squares	% variation	Fixation indices	df	Sum of squares	% variation	Fixation index
Assuming no regional differentiation	Among populations	43	1088.015	87.30	Φ_{ST} = 0.873*	41	799.131	88.19	Φ_{ST} = 0.881*
	Within populations	172	125.467	12.70		117	78.208	11.81	
Assuming regional differentiation	Among western-central group[1]	1	6.407	4.73	F_{SC} = 0.869*	1	279.626	46.02	F_{SC} = 0.830*
	Among populations within groups[1]	42	1031.607	82.87	Φ_{ST} = 0.875*	40	519.505	44.85	Φ_{ST} = 0.909*
	Within populations	172	25.467	12.41	F_{CT} = 0.047	117	78.208	9.14	F_{CT} = 0.460*
	Among geographical groups[2]	9	858.858	68.52	F_{SC} = 0.630*	9	572.473	59.13	F_{SC} = 0.728*
	Among populations within groups[2]	34	229.157	19.83	Φ_{ST} = 0.884*	32	226.658	29.76	Φ_{ST} = 0.889*
	Within populations	172	125.467	11.65	F_{CT} = 0.685*	117	78.208	11.10	F_{CT} = 0.591*

[1] Western-central group: Majorca, Ibiza, Alicante, Gibraltar, Morocco and Algeria belong to western group and Sardinia, Sicily, Pantelleria and Malta belong to central Mediterranean area.
[2] Geographical groups: Majorca, Ibiza, Alicante, Gibraltar, Morocco, Algeria, Sardinia, Sicily, Pantelleria and Malta.
* $p < 0.001$ (significant after 1023 permutations)

Supplementary data

Table S1. A. Location and abbreviation codes of the 44 *Helichrysum pendulum* complex populations included in this research. Geographical location of each population is shown in Figs. 1 and 2. Number of specimens included for each DNA marker are also shown. Number of individuals carrying a given haplotype and ribotype is shown in brackets. B. Location and abbreviation codes of the specimens belonging to other species included in this research. Coordinates were not available for some of the collections; in these case approximate coordinates are indicated in [ ]. Number of specimens included for each DNA marker is indicated.

Species	Country	Locality and voucher	Coordinates	Population name	Number of specimens for rpl32-trnL spacer	Number of specimens for ETS	Haplotype rpl32-trnL spacer	Ribotype ETS
A. *HELICHRYSUM PENDULUM* COMPLEX								
Helichrysum errerae Tineo	Italy	Sicily, Pantelleria island, close to Pantelleria village, *Galbany 2324* (BC)	36º 49' 29,0" N 11º 55' 54,0" E	E1	5	5	H1 (5)	R41 (5)
		Sicily, Pantelleria island, close to Cala 5 Denti, *Galbany 2327* (BC)	36º 49' 11,8" N 11º 59' 58,5" E	E2	6	6	H1 (6)	R41 (6)
		Sicily, Pantelleria island, between Scauri and Balata d. Turchi, *Galbany 2325* (BC)	36º 45' 09,7" N 11º 58' 47,9" E	E3	6	6	H1 (6)	R41 (5), R42(1)
Helichrysum pendulum (C. Presl) C. Presl	Spain	Balearic islands, Majorca, Formentor, by the road to Albercutx tower, *Sáez s.n.*(BC)	39º 55' 35,49" N 3º 06' 41,80" E	P1	5	5	H1 (5)	R14 (2), R15 (3)
		Balearic islands, Majorca, Gorg Blau, *Sáez s.n.* (BC)	39º 48' 30,78" N 2º 49' 13,28" E	P2	5	4	H1 (3), H10 (2)	R8 (4)
		Balearic islands, Majorca, Randa, *Sáez s.n.* (BC)	39º 31' 13,33" N 2º 55' 35,95" E	P3	5	4	H1 (5)	R14 (3), R19 (1)
		Balearic islands, Cabrera archipelago, Imperialet, *Sáez s.n.* (BC)	39º 07' 42,09" N 2º 57' 23,87" E	P4	5	4	H1 (5)	R13 (4)
		Balearic islands, Ibiza, by the way to Cala Xarraca, *Galbany 2245 & Arrabal* (BC)	39º 05' 37,8" N 1º 29' 57" E	P5	6	2	H1 (5), H8 (1)	R11 (1), R14 (1)
		Balearic islands, Ibiza, Santa Agnès de Corona, by the way to Cala Aubarca, *Galbany 2244 & Arrabal* (BC)	39º 03' 41,5" N 1º 22' 40,5" E	P6	6	8	H1 (6)	R11 (1), R14 (7)
		Balearic islands, Ibiza, Santa Agnès de Corona, by the way to Cala Ses Balandres, *Galbany 2256 & Arrabal* (BC)	39º 02' 49,6" N 1º 19' 27,8" E	P7	5	4	H1 (5)	R8 (1), R12 (1), R14 (1), R19 (1)
		Balearic islands, Ibiza, Vedranell, *Sáez s.n.*(BC)	38º 52' 07,19" N 1º 12' 30,20" E	P8	1	1	H1 (1)	R11 (1)
		Balearic islands, Ibiza, Es Vedrà, *Sáez s.n.* (BC)	38º 52' 01,68" N 1º 11' 55,21" E	P9	1	1	H1 (1)	R14 (1)
		Rock of Gibraltar, *Galbany 2191 & Arrabal* (BC)	36º 08' 47,65" N 5º 20' 43,92" W	P10	5	5	H10 (3), H11 (2)	R28 (5)
	Morocco	Rif mountains, Djebel Tassaout, between Talambote and Djebel Tassaout, *Galbany 2297 & al.*(BC)	35º 15' 52,1" N 5º 07' 29,5" W	P11	5	5	H10 (5)	R18 (2), R26 (1), R32 (2)
		Middle Atlas, between Sefrou and Ifrane, *Galbany 2298 & al.* (BC)	33º 37' 51,8" N 4º 54' 16,2" W	P12	5	3	H1 (5)	R17 (3)
		Beni-Mellal, El-Ksiba, *Galbany 2220 & al.* (BC)	32º 32' 04,4" N 6º 00' 54,3" W	P13	5	5	H1 (5)	R16 (3), R18 (1), R20 (1)
	Algeria	Oran, route of Santa Cruz, *Vela 5* (no voucher available)	35° 42' 39" N 0° 39' 54" W	P14	6	4	H1 (4), H5 (2)	R7 (1), R9 (2), R16 (1)
		Djurdjura, Azrou n'Tohor, *Vela 9* (BC)	36° 29' 19" N 4° 23' 18" E	P15	5	5	H1 (5)	R18 (5)
		Djurjura, Col de Tirourda, *Aldasoro 20093* (BC)	36º 28' 29" N 4º 21' 13" E	P16	6	5	H1 (4), H9 (2)	R18 (5)
		Bejaia, Cap Carbon, *Vela 2* (no voucher available)	36° 46' 12" N 5° 06' 15" E	P17	2	0	H1 (2)	—
		Bejaia, Pic des Singes, col, *Vela 4* (no voucher available)	36° 46' 10" N 5° 05' 43" E	P18	6	5	H1 (6)	R5 (1), R6 (1), R7 (1), R10 (2)
		Annaba, La Volie Noire, *Vela 6* (no voucher available)	36° 57' 37" N 7° 41' 26" E	P19	4	2	H1 (4)	R23 (2)
	Italy	Sardinia, pr. Oliena, *Galbany 2084 & Arrabal* (BC)	40º 15' 26,5" N 9º 25' 5,3" E	P20	5	4	H12 (5)	R33 (3), R34 (1)
		Sardinia, road between Grotta Ispinigoli and Cala Gonone, *Galbany 2078 & Arrabal* (BC)	40º 17' 59,8" N 9º 37' 58,4" E	P21	5	0	H14 (5)	—
		Sardinia, between Genna Silana and Urzulei, *Galbany 2082 & Arrabal* (BC)	40º 06' 4,5" N 9º 30' 43,8" E	P22	6	2	H12 (6)	R33 (2)
		Sardinia,road between Baunei and San Pietro, *Galbany 2083 & Arrabal* (BC)	40º 03' 55,7" N 9º 40' 1,4" E	P23	2	3	H13 (2)	R33 (1), R34 (1), R35 (1)
		Sardinia, Ulassai, *Carnicero 390 & Galbany* (BC)	39º 48' 30,06" N 9º 29' 52,01" E	P24	5	1	H14 (5)	R44 (1)
		Sicily, Marettimo islet, by the way to Punta Troia, *Galbany 2328 & Garcia* (BC)	37º 58' 24,4" N 12º 4' 05,0" E	P25	5	2	H1 (1), H2 (4)	R37 (1), R43 (1)
		Sicily, San Vito lo Capo, prop de Torre dell'Impiso, *Galbany 2329 & Garcia* (BC)	38º 08' 35,7" N 12º 46' 14,5" E	P26	6	4	H1 (5), H6 (1)	R39 (4)
		Sicily, by the road from Castellammare del Golfo to Balata di Baida, *Vilatersana 1161 & al.* (BC)	38º 1' 56" N 12º 52' 16" E	P27	6	1	H1 (6)	R39 (1)
		Sicily, Palermo, Sferracavallo, *Galbany 2321 & Garcia* (BC)	38º 12' 03,5" N 13º 16' 02,8" E	P28	7	5	H1 (7)	R34 (1), R36 (1), R39 (3)
		Sicily, Palermo, Monte Pellegrino, *Galbany 2322 & Garcia* (BC)	38º 09' 23,0" N 13º 22' 02,6" E	P29	5	5	H1 (5)	R39 (5)
		Sicily, Bagheria, Capo Zafferano, *Galbany 2319 & Garcia* (BC)	38º 06' 40,4" N 13º 32' 22,0" E	P30	6	2	H1 (6)	R34 (1), R39 (1)
		Sicily, dirty road from Portella della Páglia to La Pizzuta, *Galbany 2309 & Garcia* (BC)	37º 59' 38,6" N 13º 15' 03,0" E	P31	2	1	H2 (2)	R27 (1)
		Sicily, Madonie mountains, Isnello, road from Cefalu to Isnello, *Susanna & Garcia 2774* (BC)	37º 55' 18,68" N 14º 00' 06,73" E	P32	6	4	H2 (6)	R38 (2), R39 (2)
		Sicily, Madonie, parco regionale delle Madonie, crest of Mount Quacella, by the way to Vallone Madonna delle Angeli, *Vilatersana 1154 & al.* (BC)	37º 50' 42" N 14º 0' 53" E	P33	5	4	H2 (5)	R34 (3), R39 (1)
		Sicily, between Avola and Avola Vecchia, *Susanna & Garcia 2771* (BC)	36º 55' 17,11" N 15º 08' 30,75" E	P34	6	4	H1 (3), H3 (3)	R21 (4)
		Sicily, between Modica and Ragusa, *Susanna & Garcia 2772* (BC)	36º 53' 39,28" N 14º 45' 02,91" E	P35	5	4	H1 (1), H3 (1), H4 (3)	R21 (2), R22 (1), R40 (1)
	Malta	Gozo island, San Lawrenz, *Galbany 2263 & Arrabal* (BC)	36º 03' 46,9" N 14º 11' 27,1" E	P36	4	4	H15 (4)	R24 (3), R25 (1)
		Gozo island, Dwejra, Inland sea, *Galbany 2262 & Arrabal* (BC)	36º 03' 14,97" N 14º 11' 31,33" E	P37	5	4	H15 (5)	R24 (4)
Helichrysum valentinum Rouy	Spain	Alicante, Montgó mountain, *Galbany 2271 & al.* (BC)	38º 48' 50,68" N 0º 06' 34,33" E	V1	5	4	H1 (5)	R1 (2), R2(1), R7(1)
		Alicante, Moraira, by the way to Cala Llebeig, *Galbany 2284, 2285, 2286, 2288, 2289 & al.* (BC)	38º 41' 52,4" N 0º 09' 20,06" E	V2	5	4	H1 (5)	R29 (2), R30 (1), R31 (1)
		Alicante, Castell de Castells, Cerro de los Parados, *Galbany 2291 & al.* (BC)	38º 43' 25,91" N 0º 11' 35,48" W	V3	5	5	H1 (4), H7 (1)	R1 (5)
		Alicante, Benifato, Vall de Guadalest, *Galbany 2292 & al.* (BC)	38º 40' 23,44" N 0º 12' 24,05" W	V4	5	3	H1 (5)	R1 (1), R3 (1), R4 (1)

Species	Country	Locality and voucher	Coordinates	Abbreviation taxon code	Number of specimens for rpl32-trnL spacer	Number of specimens for ETS
B. OTHER SPECIES INCLUDED IN ANALYSES						
Sect. *Stoechadina*						
Helichrysum crassifolium (L.) D. Don	Spain	Balearic islands, Majorca, Cap de Formentor, *Galbany & Sáez s. n.* (BCN 6117)	[39º 56' 02,70" N 3º 05' 59,15" E]	*H. crassifolium*	1	1
Helichrysum heldreichii Boiss.	Greece	Crete, Sphakia, Aradena canyon, *Garnatje 134 & Luque* (BCN 6123)	[35º 14' 40,54" N 24º 04' 35,11" E]	*H. heldreichii*	0	1
Helichrysum italicum (Roth) G. Don subsp. *italicum*	Bosnia-Herzegovina	Herzegovina, pen. Neum, *Redžić & al. s. n.* (BCN 20756)	[43º 54' 54,97" N 17º 40' 31,77" E]	*H. italicum* subsp. *italicum* 1	0	1
	Croatia	Makirina, Pirovac, Šibenik-Knin County, *Boršić s. n.* (BC)	[43º 49' 02,12" N 15º 40' 44,69 E]	*H. italicum* subsp. *italicum* 2	1	1
	Italy	Toscana, Grosseto, road from Mascherino to Convento Padri Passionati, *Vilatersana 1229 & al.* (BC)	42º 25' 5" N 11º 9' 36" E	*H. italicum* subsp. *italicum* 3	1	1
Helichrysum italicum subsp. *microphyllum* (Willd.) Nyman	France	Corsica, La Tonnara, beach, *Galbany 2048 & Arrabal* (BC)	41º 25' 33,9" N 9º 6' 19,4" E	*H. italicum* subsp. *microphyllum* 1	1	0
	Spain	Balearic islands, Majorca, Coll d'es Telègraf, *Galbany & Sáez s. n.* (BCN 6115)	39º 48' 14,45" N 2º 50' 53,51" E	*H. italicum* subsp. *microphyllum* 2	0	1
	Spain	Balearic Islands, Dragonera, *Sáez 6991* (BC)	39º 35' 02,21" N 2º 19' 16,81" E	*H. italicum* subsp. *microphyllum* 3	0	1
Helichrysum italicum subsp. *siculum* (Jord. & Fourr.) Galbany, L. Sáez & Benedí	Italy	Sicily, Palermo, *Vilatersana 1172 & al.* (BC)	38º 0' 38" N 14º 10' 36" E	*H. italicum* subsp. *siculum* 1	1	0
		Sicily, Messina, Novara di Sicilia to Francavilla di Sicilia, *Vilatersana 1176 & al.* (BC)	37º 58' 39,36" N 15º 08' 37,26" E	*H. italicum* subsp. *siculum* 2	1	0
Helichrysum litoreum Guss.	Italy	Lipari, S of Cava del Pomice, by the road to Porticello, *Vilatersana & al. 1182* (BC)	38º 30' 17" N 141º 57' 44" E	*H. litoreum* 1	1	1
		Lazio, Latina, isole Ponziane, Isola di Ventotene, *Vilatersana & al 1114* (BC)	40º 47' 51" N 13º 25' 41" E	*H. litoreum* 2	0	1
		Lazio, Latina, S. Felice Circeo, via del Faro, *Vilatersana & al. 1105* (BC)	41º 13' 38" N 13º 5' 22" E	*H. litoreum* 3	1	1
Helichrysum stoechas (L.) Moench	Greece	Crete, Thripti, *Galbany 2143 & al.* (no voucher available)	35º 05' 15,8" N 25º 51' 37,5" E	*H. stoechas* 1	1	0
		Crete, Thripti, *Galbany 2144 & al.* (no voucher available)	35º 05' 15,8" N 25º 51' 37,5" E	*H. stoechas* 2	1	1
		Crete, Paleokastro, *Galbany 2154 & al.* (BC)	35º 23' 28,6" N 25º 02' 03,0" E	*H. stoechas* 3	1	1
		Crete, Paleokastro, *Galbany 2157 & al.* (BC)	35º 23' 28,6" N 25º 02' 03,0" E	*H. stoechas* 4	1	1
		Rhodes, between Kritinia and Siana, *Galbany 2172 & al.* (BC)	36º 12' 29,1" N 27º 48' 43,7" E	*H. stoechas* 5	1	1
	Spain	Alicante, Marina Alta, Teulada, Benimarco, *Galbany & al. 2293* (BC)	38º 42' 33,5" N 0º 05' 38,4" E	*H. stoechas* 6-1 and *H. stoechas* 6-2	1	2
		Alicante, Finestrat, Puig Campana, *Galbany 2294 & al.* (BC)	38º 35' 25,8" N 0º 12' 28,3" W	*H. stoechas* 7	0	1
		Balearic Islands, Ibiza, Vedranell, *Sáez s.n.* (BC)	38º 52' 07,19" N 1º 12' 30,20" E	*H. stoechas* 8	1	1
		Balearic Islands, Ibiza, by the road between Cala Xarraca and St. Miquel, *Galbany 2246 & Arrabal* (BC)	39º 05' 37,8" N 1º 29' 57" E	*H. stoechas* 9	1	1
		Balearic Islands, Ibiza, Santa Agnès de Corona, by the way to Cala Aubarca, *Galbany 2232 & Arrabal* (BC)	39º 03' 41,5" N 1º 22' 40,5" E	*H. stoechas* 10	0	1
		Lleida, la Granadella, *Galbany s. n.* (BCN 6114)	[41º 21' 20,93" N 0º 40' 03,64" E]	*H. stoechas* 11	1	1
Other sections						
Anaphalis margaritacea (L.) Benth. & Hook.f.	Canada	West Canada, *Blanco & Blanco s.n.* (BC)	not available	*Anaphalis margaritacea*	1	1
Helichrysum argyrosphaerum DC.	South Africa	Free State Province, *Koekemoer 3532* (BC)	not available	*H. argyrosphaerum*	1	1
Helichrysum armenium (L.) Moench	Turkey	Adiyaman, new road Katha - Nemrud Dagı , *Susanna 2346* & *al.* (BCN 6127)	[37º 53' 00,18" N 38º 34' 22,30" E]	*H. armenium*	0	1
Helichrysum arwae J. R. I. Wood	Yemen	Jebel Taaqa, Ex Roy. Bot. Gard., *Kew s.n.* (BCN 6103)	[13º 54' 40,20" N 44º 08' 06,36" E]	*H. arwae*	1	1
Helichrysum citrispinum Del.	Ethiopia	Mount Choke, *Aldasoro 9952 & Alarcón* (BC)	[10º 42' 13,34" N 37º 50' 56,86" E]	*H. citrispinum*	1	1
Helichrysum devium J. Y. Johnson	Portugal	Madeira island, Ponta de São Lourenço, *Jardim s. n.* (MADJ)	[32º 44' 09,86" N 16º 40' 11,00" W]	*H. devium*	1	1
Helichrysum foetidum (L.) Moench	South Africa	Ex Dresden Bot. Gard. (BCN 8219)	not available	*H. foetidum*	1	1
Helichrysum gossypinum Sch. Bip.	Spain	Canary Islands, Lanzarote, Máguez, La Pescosa, *Galbany & Arrabal s. n.* (BCN 25226)	[29º 10' 04,24" N 13º 30' 19,91" W]	*H. gossypinum*	1	1
Helichrysum litorale H. Bol.	South Africa	Eastern Cape Province, *Romo 14500 & al.* (BC 867722)	33º 36' 00,71" S 26º 53' 48,88" E	*H. litorale*	1	1
Helichrysum marginatum DC.	South Africa	Eastern Cape Province, between Rhodes and Naudesnek, *Romo 14434 & al.* (BC 867675)	30º 45' 32,70" S 28º 06' 12,76" E	*H. marginatum*	1	1
Helichrysum melaleucum Rchb. ex Holl	Portugal	Madeira island, Pico do Facho, *Jardim s. n.* (MADJ)	[32º 43' 45,57" N 16º 45' 44,18" W]	*H. melaleucum*	1	1
Helichrysum monizii Lowe	Portugal	Madeira island, Cabo Girão, *Jardim s. n.* (MADJ)	[32º 39' 26,67" N 17º 00' 19,54" W]	*H. monizii*	1	1
Helichrysum monogynum B. L. Burtt & Sunding	Spain	Canary Islands, Lanzarote, San Bartolomé, *Galbany & Arrabal s. n.* (BCN 25227)	[28º 59' 16,24" N 13º 36' 02,89" W]	*H. monogynum*	1	1
Helichrysum montanum DC.	South Africa	Kwazulu-Natal Province, *Romo 14392 & al.* (BC 867659)	30º 14' 40,28" S 29º 05' 43,47" E	*H. montanum*	1	1
Helichrysum mussae Nevski	Tadzhikistan	Zeravshchan mts., *Filatov 81 & al.* (LE)	not available	*H. mussae*	1	1
Helichrysum obconicum DC.	Portugal	Madeira island, Porto Novo, *Jardim s. n.* (MADJ)	[32º 39' 48,91" N 16º 48' 21,36" W]	*H. obconicum*	1	1
Helichrysum orientale (L.) Gaertn.	Greece	Crete, below Thripti, Ex Roy. Bot. Gard. Kew (BCN 6098)	35º 05' 15,8" N 25º 51' 37,5" E	*H. orientale*	1	1
Helichrysum plicatum DC.	Turkey	Sivas, 11 Km N of Zara to Şerefiye, *Susanna 2419 & al.* (BCN 6129)	[39º 54' N 37º 45' E]	*H. plicatum*	0	1
Helichrysum rubicundum (K. Koch) Bornm.	Iran	Azarbaidjan, entre Mianeh & Kivi, 4 km N de Top-Ghara, *Termeh & al. s. n.* (IRAN 35924,4)	[37º 30' 21,81" N 47º 58' 48,47" E]	*H. rubicundum*	1	1
Helichrysum rugulosum Less.	South Africa	Free State Province, *Romo 14331 & al.* (BC 867613)	27º 39' 13,64" S 28º 30' 47,32" E	*H. rugulosum*	1	1
Helichrysum sibthorpii Rouy	Greece	Mt. Athos. Ex Roy. Bot. Gard., *Kew s.n.* (BCN 6099)	[40º 09' 23,66" N 24º 19' 26,86" E]	*H. sibthorpii*	1	1
Helichrysum thianschanicum Regel		Ex hort. Hortus Botanicus Táhor (BCN 10337)	not available	*H. thianschanicum*	1	1

Figure captions

Fig. 1. A. Geographic distribution and parsimony network relationships of the 15 different haplotypes found in 216 individuals belonging to the three species of the *Helichrysum pendulum* complex. For population abbreviation codes and additional information see Table S1. The arrows indicate the locations of the 44 sampled populations. The size of circles is proportional to the frequency of each haplotype in the total sample. Small black circles represent intermediate haplotypes that were not detected and each line in the network represents one mutational step. **B.** Phylogram obtained from Bayesian analysis of the 15 haplotypes detected in the *Helichrysum pendulum* complex and four additional *Helichrysum* species coded as outgroup taxa (dataset 1). Bayesian Posterior Probabilities are shown above branches and Bootstrap values from Maximum Parsimony analysis are shown below branches. Colour codes are the same as in A.

Fig. 2. A Geographic distribution of the 44 different ribotypes found in 159 individuals belonging to the three species of the *Helichrysum pendulum* complex. For population abbreviation codes and additional information see Table 1. The arrows indicate the locations of the 42 sampled populations. **B.** Unrooted phylogenetic tree obtained from Bayesian analysis of the 44 ribotypes detected in the *Helichrysum pendulum* complex and four additional *Helichrysum* species coded as outgroup taxa (dataset 3). Bayesian Posterior Probabilities are shown above branches and Bootstrap values from Maximum Parsimony analysis are shown below branches. Colour codes are the same as in A.

Fig. 3. A. BAPS analysis of all populations of the *Helichrysum pendulum* complex using cpDNA sequences (K=2). **B**. BAPS analysis of all populations of the *Helichrysum pendulum* complex using nrDNA ETS sequences (K =3). **C.** The first five barriers detected in the *H. pendulum* complex using BARRIER software with cpDNA sequences using Nei's genetic distances. The polygons result from the Voronoi tessellation. **D**. The first five barriers detected in the *H. pendulum* complex using BARRIER software with nrDNA ETS sequences using Nei's genetic distances. The polygons result from the Voronoi tessellation.

Fig. 4. Phylogram obtained from Bayesian analysis of the 15 haplotypes detected in the *Helichrysum pendulum* complex and the rest of the species included in the study (dataset 2, see text for details). Bayesian Posterior Probabilities are shown above branches and Bootstrap values from Maximum Parsimony analysis are shown below branches. Colour codes are the same as in Fig. 1.

Fig. 5. Phylogram obtained from Bayesian analysis of the 44 ribotypes detected in the *Helichrysum pendulum* complex and the rest of the species included in the study (dataset 4, see text for details). Bayesian Posterior Probabilities are shown above branches and Bootstrap values from Maximum Parsimony analysis are shown below branches. Colour codes are the same as in Fig. 2.

Fig. 6. Neighbour-net graph derived from the 44 ribotypes detected in the *Helichrysum pendulum* complex and other taxa also belonging to sect. *Stoechadina* (see text for details), with locality showed in brakets. Additional information on the specimens bearing each ribotype and on taxon abbreviation codes is specified in Table S1.

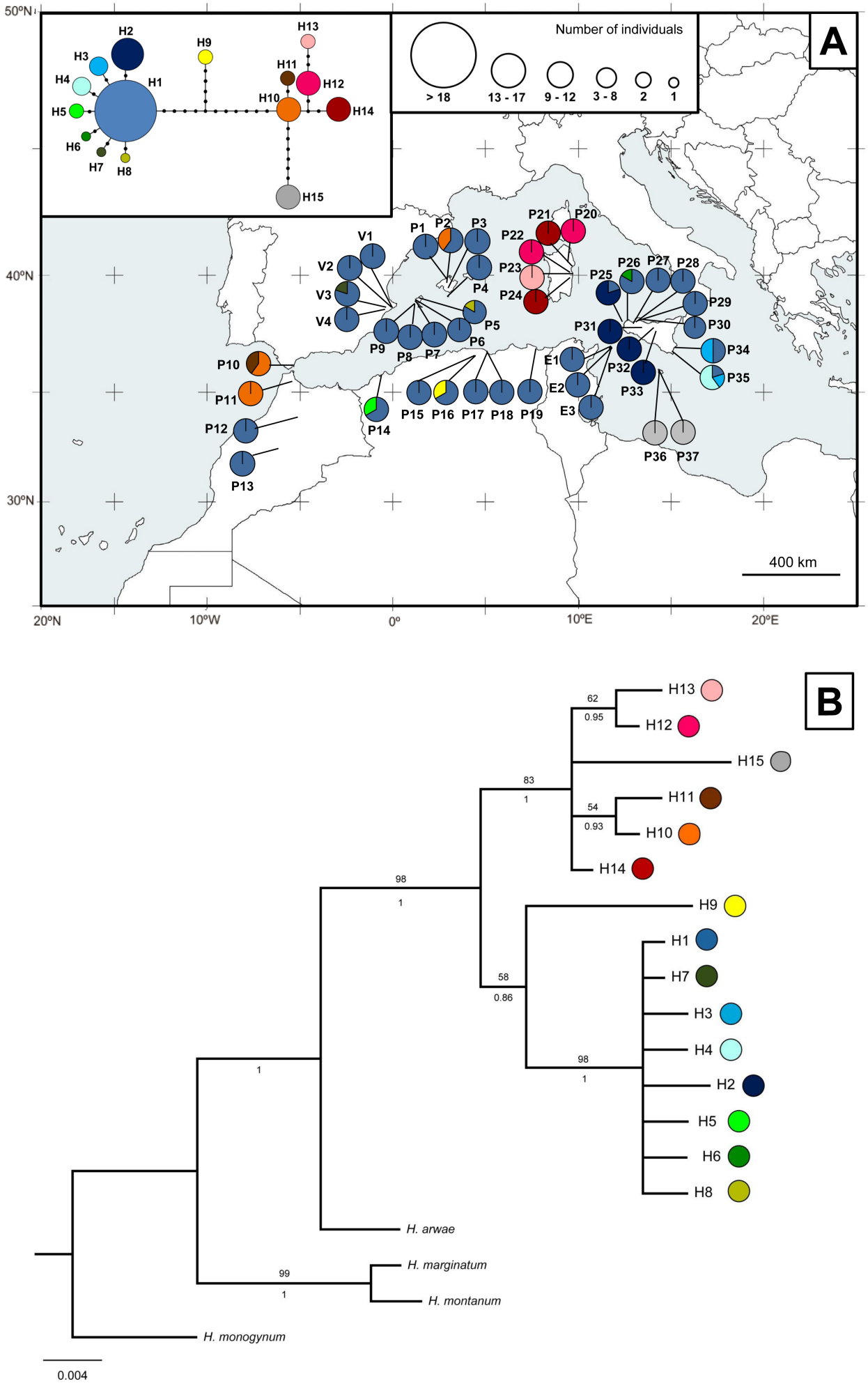
A
Number of individuals
> 18
13 - 17
9 - 12
3 - 8
2
1
H1
H2
H3
H4
H5
H6
H7
H8
H9
H10
H11
H12
H13
H14
H15
V1
V2
V3
V4
P1
P2
P3
P4
P5
P6
P7
P8
P9
P10
P11
P12
P13
P14
P15
P16
P17
P18
P19
P20
P21
P22
P23
P24
P25
P26
P27
P28
P29
P30
P31
P32
P33
P34
P35
P36
P37
E1
E2
E3
400 km
50°N
40°N
30°N
20°N
10°W
0°
10°E
20°E
B
H13
H12
H15
H11
H10
H14
H9
H1
H7
H3
H4
H2
H5
H6
H8
62
0.95
83
1
54
0.93
98
1
58
0.86
98
1
1
99
1
H. arwae
H. marginatum
H. montanum
H. monogynum
0.004

Fig. 1.

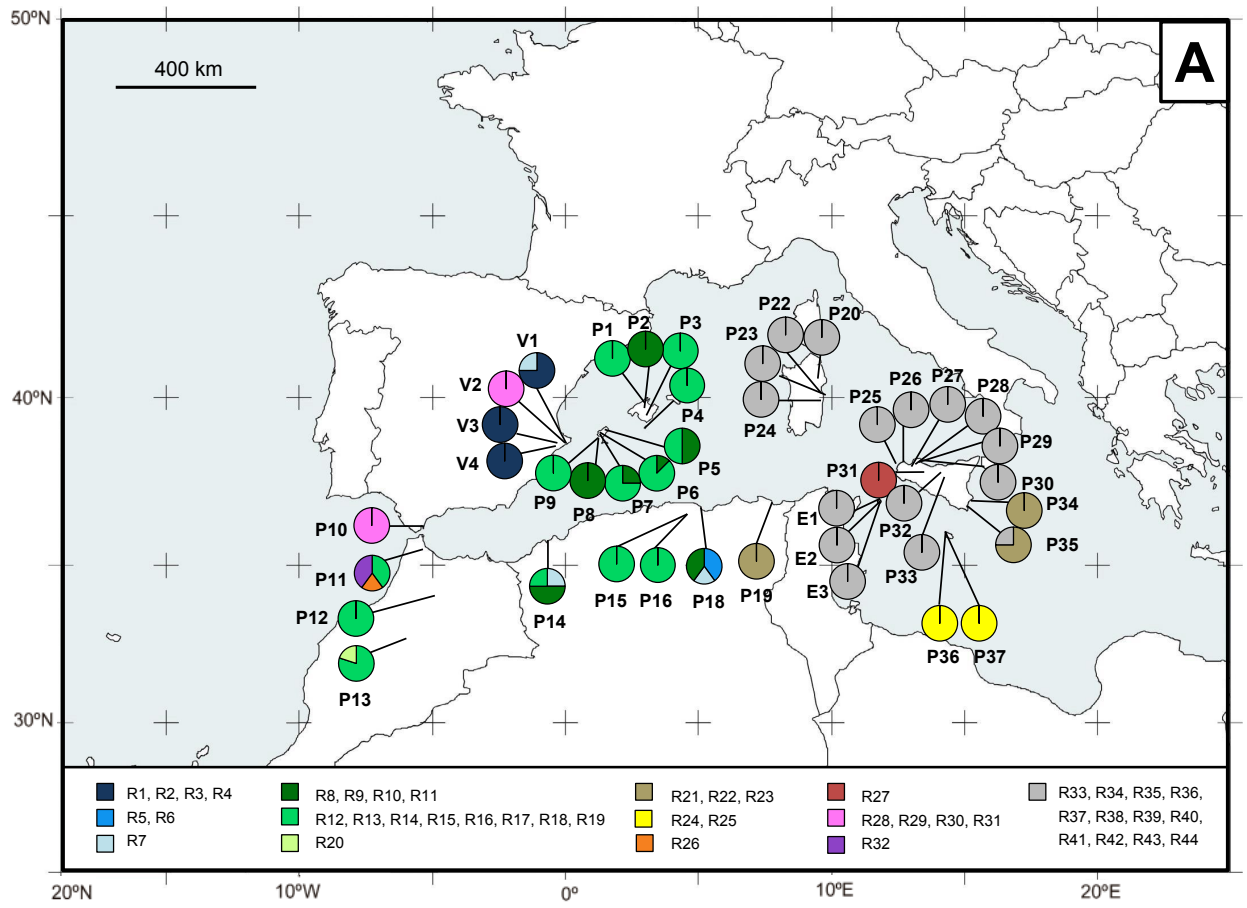
A
400 km
50°N
40°N
30°N
20°N
10°W
0°
10°E
20°E
V1
V2
V3
V4
P1
P2
P3
P4
P5
P6
P7
P8
P9
P10
P11
P12
P13
P14
P15
P16
P18
P19
P20
P22
P23
P24
P25
P26
P27
P28
P29
P30
P31
P32
P33
P34
P35
P36
P37
E1
E2
E3
R1, R2, R3, R4
R5, R6
R7
R8, R9, R10, R11
R12, R13, R14, R15, R16, R17, R18, R19
R20
R21, R22, R23
R24, R25
R26
R27
R28, R29, R30, R31
R32
R33, R34, R35, R36, R37, R38, R39, R40, R41, R42, R43, R44

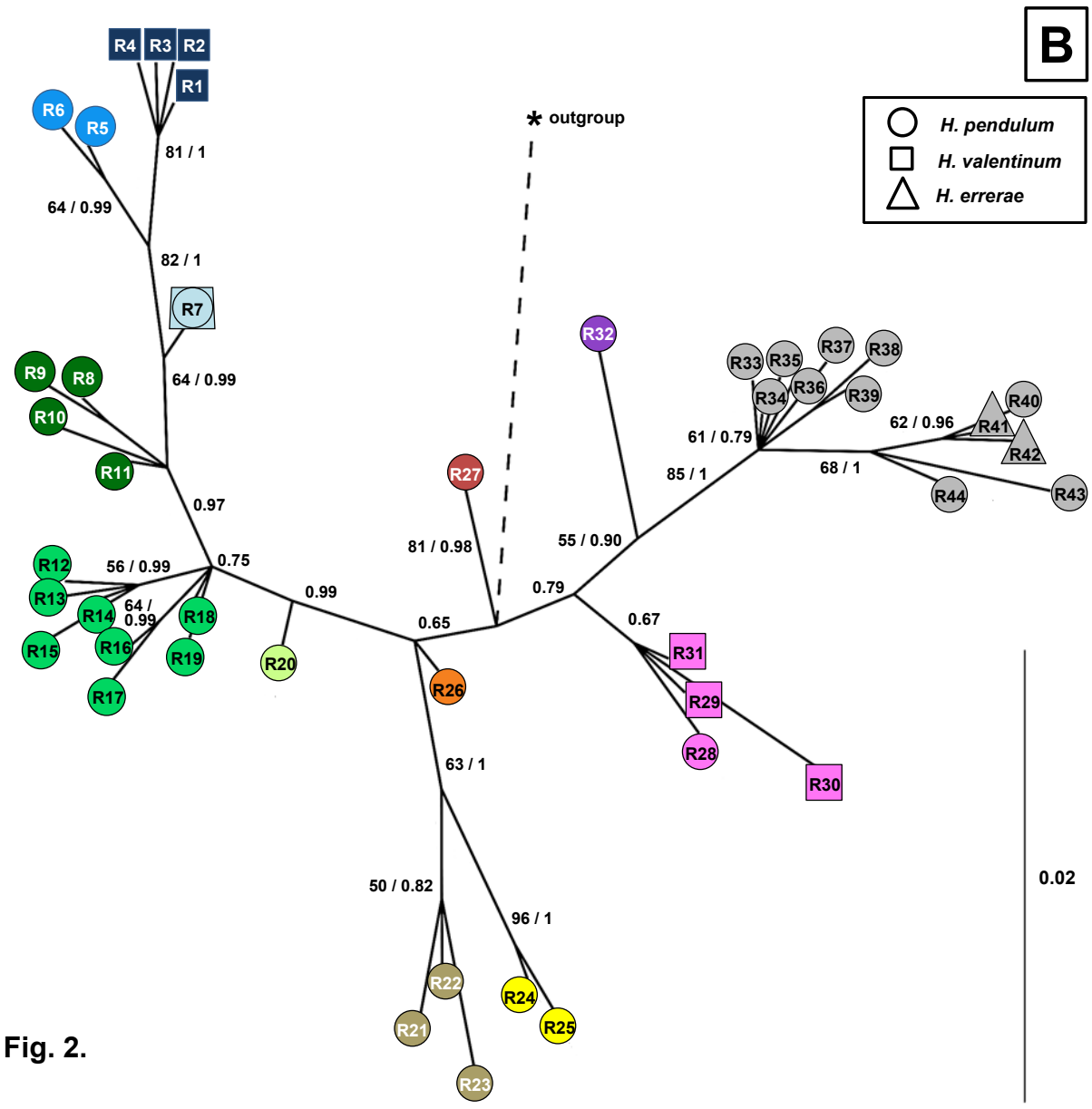
B
H. pendulum
H. valentinum
H. errerae
* outgroup
R4
R3
R2
R1
R6
R5
81 / 1
64 / 0.99
82 / 1
R7
64 / 0.99
R9
R8
R10
R11
0.97
R12
56 / 0.99
R13
R14
64 / 0.99
R15
R16
R17
R18
R19
0.75
R20
0.99
0.65
81 / 0.98
R27
R26
R32
55 / 0.90
0.79
R33
R35
R37
R38
R34
R36
R39
61 / 0.79
62 / 0.96
R40
R41
R42
85 / 1
68 / 1
R44
R43
0.67
R31
R29
R28
R30
63 / 1
50 / 0.82
96 / 1
R22
R24
R25
R21
R23
0.02

Fig. 2.

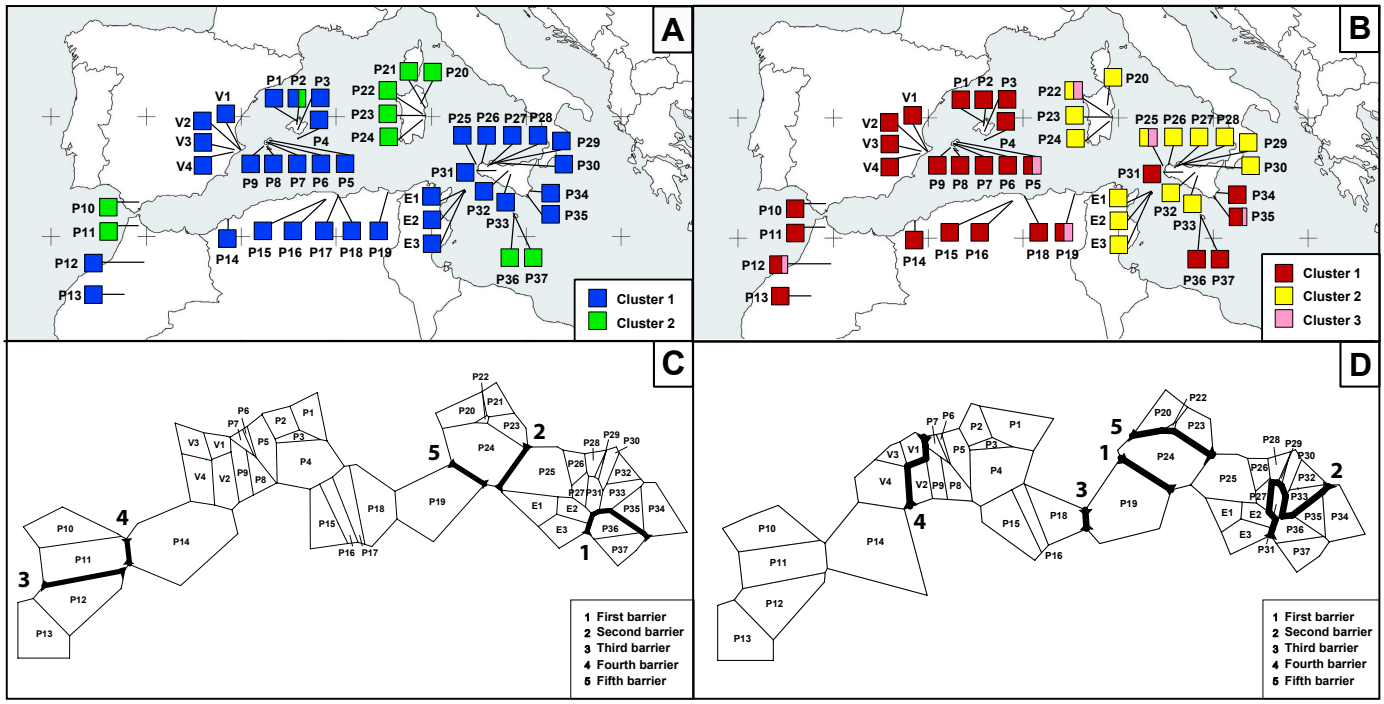
A
B
C
D
Cluster 1
Cluster 2
Cluster 3
1 First barrier
2 Second barrier
3 Third barrier
4 Fourth barrier
5 Fifth barrier

Fig. 3.

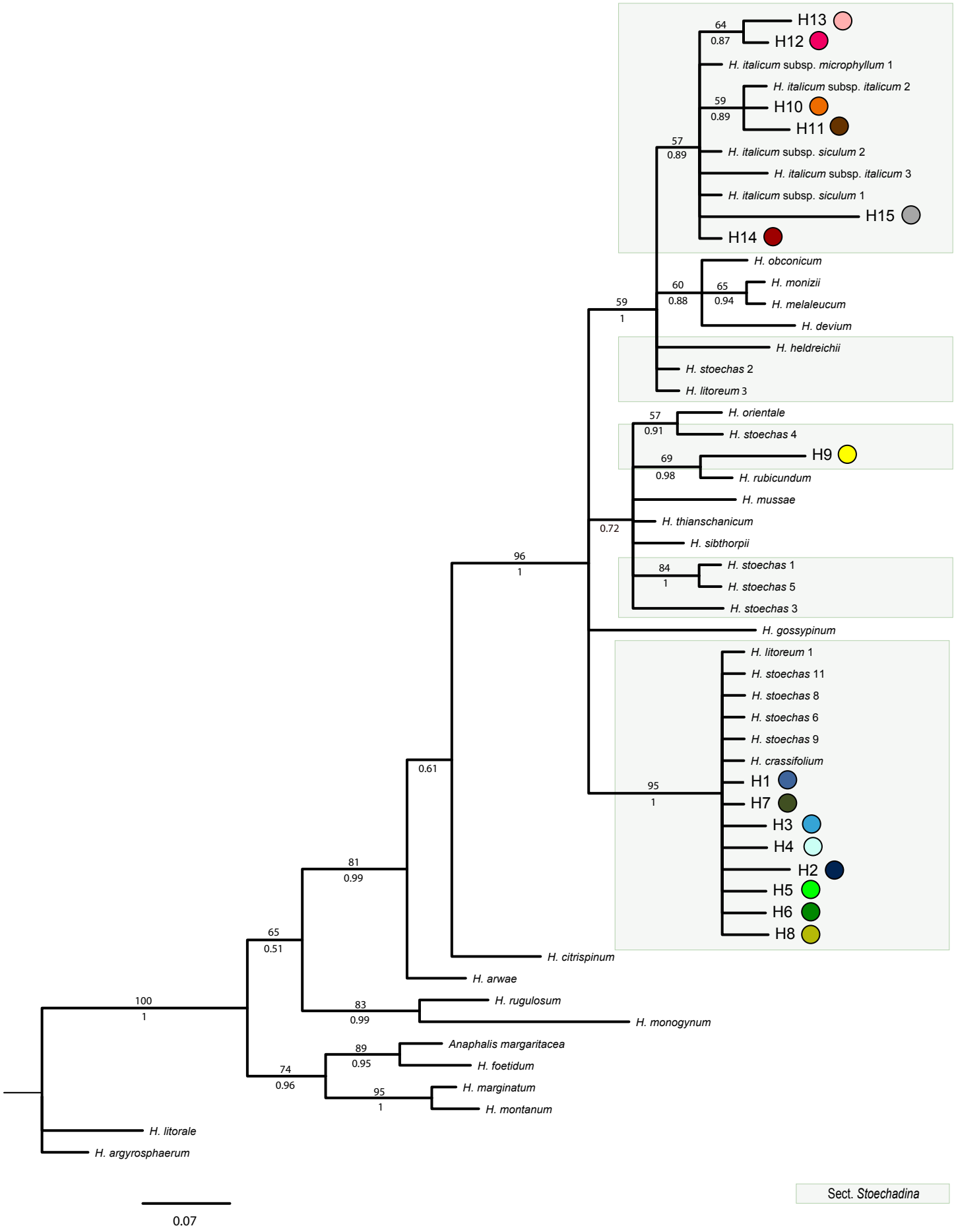
H13
H12
H. italicum subsp. microphyllum 1
H. italicum subsp. italicum 2
H10
H11
H. italicum subsp. siculum 2
H. italicum subsp. italicum 3
H. italicum subsp. siculum 1
H15
H14
H. obconicum
H. monizii
H. melaleucum
H. devium
H. heldreichii
H. stoechas 2
H. litoreum 3
H. orientale
H. stoechas 4
H9
H. rubicundum
H. mussae
H. thianschanicum
H. sibthorpii
H. stoechas 1
H. stoechas 5
H. stoechas 3
H. gossypinum
H. litoreum 1
H. stoechas 11
H. stoechas 8
H. stoechas 6
H. stoechas 9
H. crassifolium
H1
H7
H3
H4
H2
H5
H6
H8
H. citrispinum
H. arwae
H. rugulosum
H. monogynum
Anaphalis margaritacea
H. foetidum
H. marginatum
H. montanum
H. litorale
H. argyrosphaerum
64
0.87
59
0.89
57
0.89
60
0.88
65
0.94
59
1
57
0.91
69
0.98
0.72
96
1
84
1
95
1
0.61
81
0.99
65
0.51
100
1
83
0.99
89
0.95
74
0.96
95
1
0.07
Sect. Stoechadina

Fig. 4.

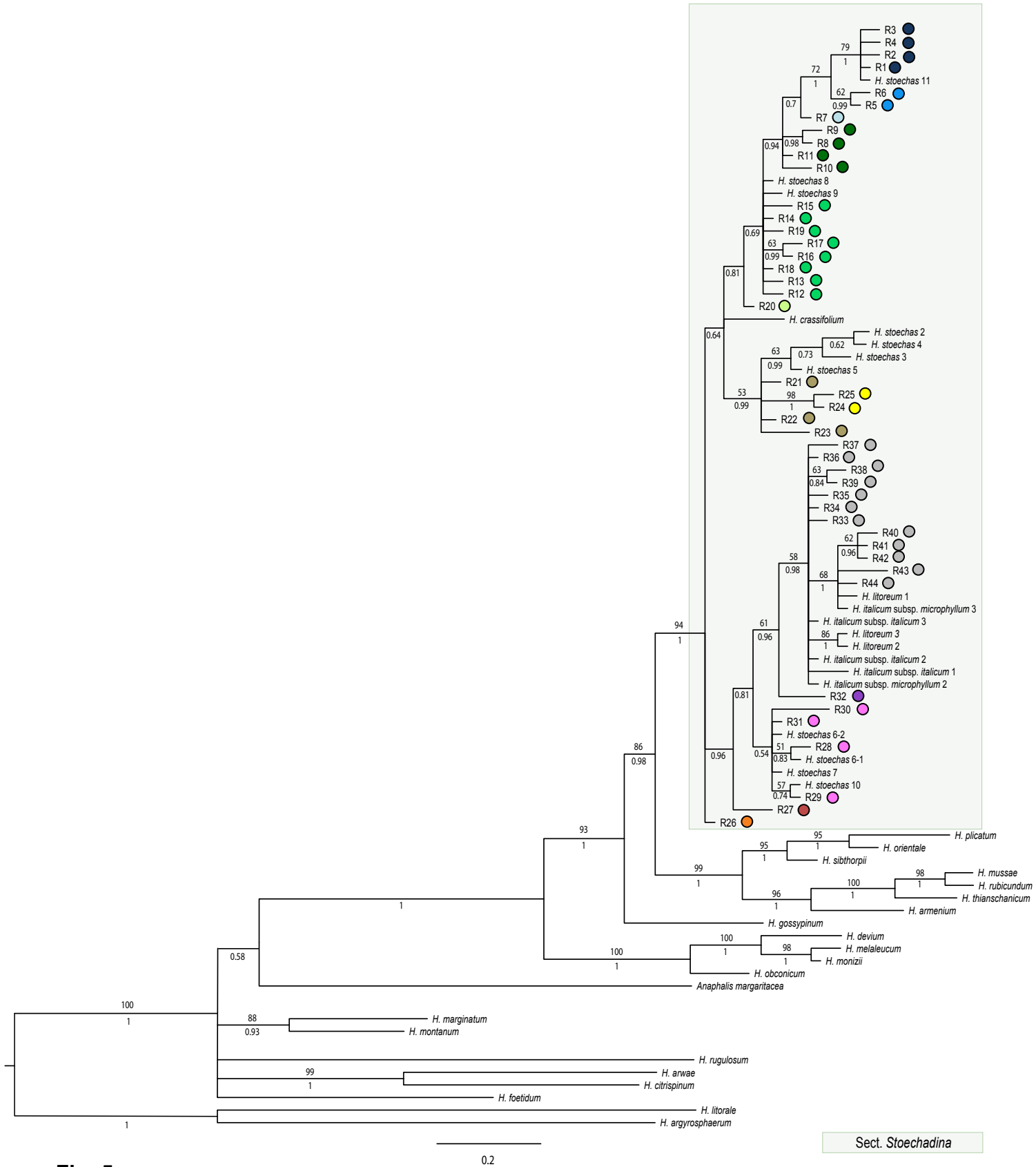
R3
R4
R2
R1
H. stoechas 11
R6
R5
R7
R9
R8
R11
R10
H. stoechas 8
H. stoechas 9
R15
R14
R19
R17
R16
R18
R13
R12
R20
H. crassifolium
H. stoechas 2
H. stoechas 4
H. stoechas 3
H. stoechas 5
R21
R25
R24
R22
R23
R37
R36
R38
R39
R35
R34
R33
R40
R41
R42
R43
R44
H. litoreum 1
H. italicum subsp. microphyllum 3
H. italicum subsp. italicum 3
H. litoreum 3
H. litoreum 2
H. italicum subsp. italicum 2
H. italicum subsp. italicum 1
H. italicum subsp. microphyllum 2
R32
R30
R31
H. stoechas 6-2
R28
H. stoechas 6-1
H. stoechas 7
H. stoechas 10
R29
R27
R26
H. plicatum
H. orientale
H. sibthorpii
H. mussae
H. rubicundum
H. thianschanicum
H. armenium
H. gossypinum
H. devium
H. melaleucum
H. monizii
H. obconicum
Anaphalis margaritacea
H. marginatum
H. montanum
H. rugulosum
H. arwae
H. citrispinum
H. foetidum
H. litorale
H. argyrosphaerum
0.2
Sect. Stoechadina

Fig. 5.

Fig. 6.

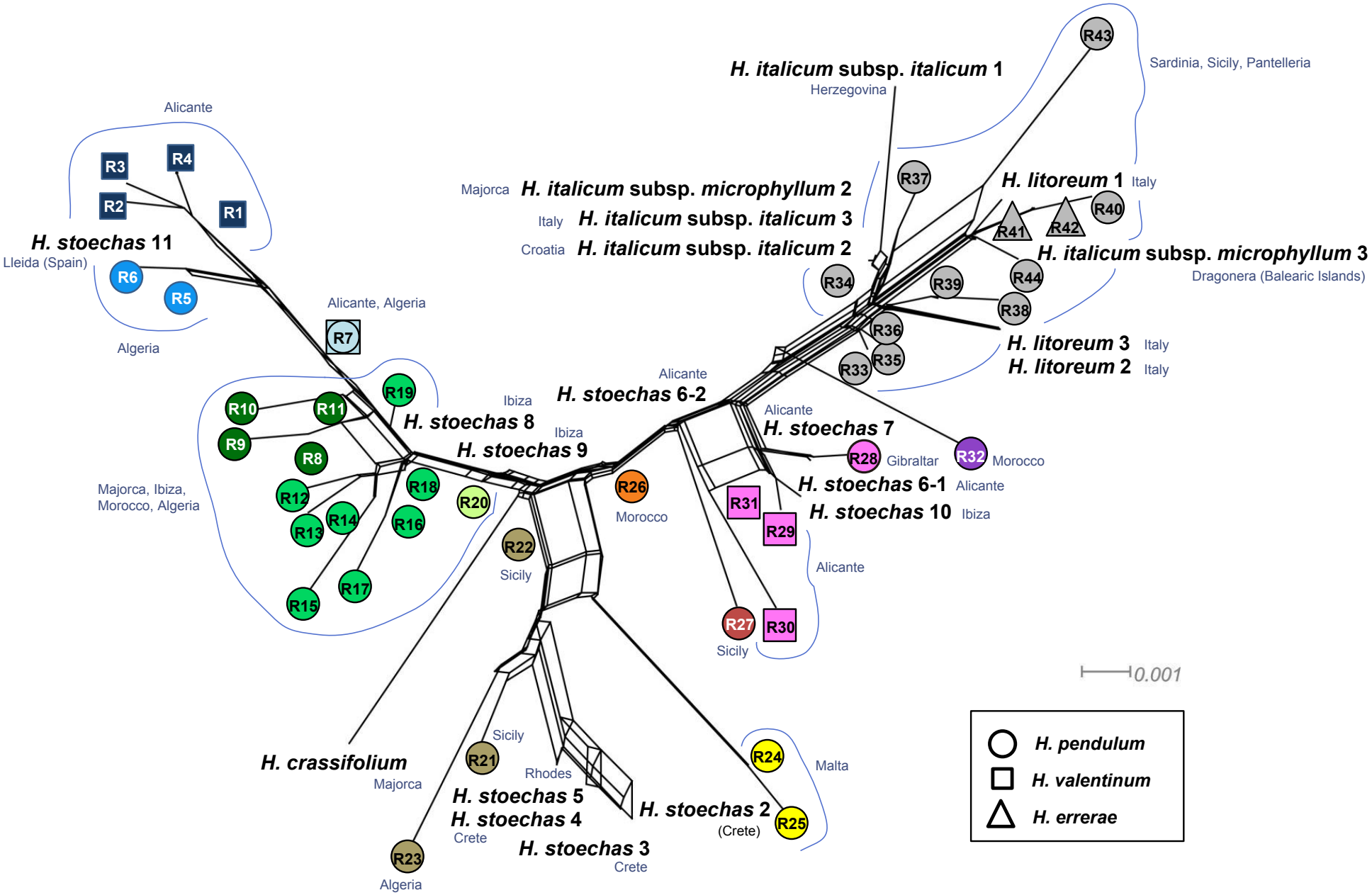
H. italicum subsp. italicum 1
Herzegovina
Sardinia, Sicily, Pantelleria
R43
Majorca H. italicum subsp. microphyllum 2
Italy H. italicum subsp. italicum 3
Croatia H. italicum subsp. italicum 2
H. litoreum 1 Italy
R37
R40
R41
R42
H. italicum subsp. microphyllum 3
Dragonera (Balearic Islands)
R34
R39
R44
R38
R36
R35
R33
H. litoreum 3 Italy
H. litoreum 2 Italy
Alicante
R3
R4
R2
R1
H. stoechas 11
Lleida (Spain)
R6
R5
Algeria
Alicante, Algeria
R7
Alicante
H. stoechas 6-2
Ibiza
R19
R10
R11
H. stoechas 8
R9
Ibiza
H. stoechas 9
R8
Majorca, Ibiza,
Morocco, Algeria
R12
R18
R20
R14
R16
R13
R17
R15
R26
Morocco
Alicante
H. stoechas 7
R28
Gibraltar
R32
Morocco
H. stoechas 6-1
Alicante
H. stoechas 10
Ibiza
R31
R29
Alicante
R22
Sicily
R27
R30
Sicily
0.001
H. pendulum
H. valentinum
H. errerae
Sicily
R21
H. crassifolium
Majorca
Rhodes
R24
Malta
H. stoechas 5
H. stoechas 4
Crete
H. stoechas 2
(Crete)
R25
H. stoechas 3
Crete
R23
Algeria